Chapter 6
Timescale Analysis

Abstract A very characteristic feature of chemical kinetic models (in common with many other models in science) is that they contain a wide range of different timescales. This may have consequences for model behaviour and also for the selection of appropriate solution methods for the resulting equation systems. Several aspects of timescales of models are therefore discussed within this chapter. The discussion begins with the definition of various simple quantities used to measure timescales, such as species half-life and species lifetime, and explores their relationship to the time-dependent behaviour of the model. Timescales are closely related to the dynamic behaviour of the model following a perturbation within the chemical kinetic system, e.g., by suddenly altered concentrations. Systematic investigation of such perturbations can be achieved for large systems using computational singular perturbation (CSP) theory which is introduced here. Another common feature of chemical kinetic models is that the chemical kinetics relaxes the system to lower and lower-dimensional attractors until either a stationary point or chemical equilibrium (zero-dimensional attractor) or other low-dimensional attractor (e.g. a limit cycle) is reached. This leads to the importance of slow manifolds in the space of variables which will be investigated within this chapter. One practically important consequence of the presence of very different timescales is the stiffness of reaction kinetic models. Methods for dealing with stiffness within numerical models are therefore discussed.

6.1 Introduction

As explained in Sect. 2.1, a full description of the time-dependent progress of a chemical reaction system requires a mechanism containing not just reactants and products but also important intermediate species. The rate of consumption of the species within the mechanism can vary over many orders of magnitude depending on the species type. Radical intermediates, for example, usually react on quicker timescales than stable molecular species. This can lead to numerical issues when attempting to solve initial value problems such as that expressed in Eq. (5.1), since the variation in timescales can lead to a stiff differential equation system which may become numerically unstable unless a small time step is used or special numerical

© Springer-Verlag Berlin Heidelberg 2014

T. Turányi, A.S. Tomlin, *Analysis of Kinetic Reaction Mechanisms*,
DOI 10.1007/978-3-662-44562-4_6

solvers are employed (Sandu et al. 1997a). On the other hand, the separation in timescales within a chemical model may be a feature that can be exploited within model reduction strategies. A simple example based on the application of the QSSA was already discussed in Sect. 2.3. We may also wish to ask questions related to the dynamic response of a chemical system. For example, we may wish to determine which species or reactions control the progress of a system towards a steady state. For these and other reasons, it can be very useful to analyse the timescales present within a chemical system using a variety of methods discussed in this chapter and in the following chapter on model reduction.

6.2 Species Lifetimes and Timescales

The simplest way to decompose the timescales of a chemical system is according to individual species. The *half-life* $\tau_{1/2}$ of a species is the time during which the concentration of a species would be halved, estimated by assuming that the investigated species is not produced, and all rate coefficients and other concentrations remain at their initial value. More specifically, only those species concentrations have to remain constant, which influence the consumption rate of the investigated species. It is clear from this definition that cases where the concentration of the species is really halved during the half-life may be exceptional ones.

Such exceptional cases usually form the examples given in textbooks. For example, when the only reaction of species A is its first-order decay $\mathrm{A} \rightarrow \mathrm{B}$ with rate coefficient k, and at initial time $t = 0$, its concentration is a_0, the change of its concentration over time is given by

$$a(t) = a_0 \exp(-kt) \tag{6.1}$$

$$\frac{a(t)}{a_0} = \exp(-kt) \tag{6.2}$$

The linearised form of this expression can be obtained by taking the natural logarithm of both sides:

$$\ln\left(\frac{a(t)}{a_0}\right) = -kt \tag{6.3}$$

After time $\tau_{1/2}$, the concentration of A will be half ($a_0/2$) of the initial value.

$$\ln\left(\frac{\frac{a_0}{2}}{a_0}\right) = \ln\left(\frac{1}{2}\right) = \ln\left(2^{-1}\right) = -\ln 2 = -k\tau_{1/2} \tag{6.4}$$

$$\tau_{1/2} = \frac{\ln 2}{k} \tag{6.5}$$

This means that in a first-order decay, the half-life is independent of the initial concentration.

If the only reaction of species A is its second-order decay $2\mathrm{A} \rightarrow \mathrm{B}$ with rate coefficient k', and the initial concentration is a_0 at time $t = 0$, then the corresponding concentration−time function is

$$\frac{1}{a(t)} = \frac{1}{a_0} + 2k' t \tag{6.6}$$

Introducing notation $k = 2k'$, the half-life is

$$\frac{1}{a_0/2} = \frac{2}{a_0} = \frac{1}{a_0} + k\,\tau_{1/2} \tag{6.7}$$

$$\tau_{1/2} = \frac{1}{k\,a_0} \tag{6.8}$$

Therefore, for a second-order decay, the time to reach half of a given concentration depends on the actual concentration a_0.

These simple textbook examples can be misleading, since in these cases, the concentration is really halved after time $\tau_{1/2}$. In more general cases, the concentration of a species may increase, decrease or remain constant over a given half-life as it is produced and consumed in a variety of reaction steps. The calculation of half-lives can support a useful way of thinking, however, where the species under investigation is not produced in the system, is not emitted to the system, and its decay rate does not change over time. For example, in a nuclear accident, two dangerous isotopes are iodine ^{131}I (half-life 8.05 days) and caesium ^{137}Cs (half-life 30.1 years). After a time period of seven times the half-life, the amount of emitted isotopes decreases by $2^7 = 128$ times. This is 56 days for the iodine isotope and 210 years for the caesium isotope. This means that environmental problems caused by the iodine isotope are eliminated after a few months, but the problems caused by the radioactive caesium isotope may persist for several centuries. In this case then, the half-life provides a useful basis for comparison between the two isotopes. Note that the radioactive half-lives characterise the total amount of the emitted isotope and not its local concentration in air, soil or water. The decrease in concentration may be much more significant due to dilution and deposition effects. Thinking in terms of species half-lives is popular, because it is easy to imagine the amount of a species being halved, whilst it is much harder to imagine a decrease, e.g., by 2.71828 times.

In the case of many dynamical processes, the rate of change of a quantity is linearly proportional to the same quantity. Such processes include first-order decays in chemistry or radioactive decays in physics. The change of the quantity can then be described by an exponential function as shown in Eq. (6.1), and therefore the rate of change can be characterised by the time period needed to decrease the original quantity by e, where e is the basis of the natural logarithm having an approximate value of 2.71828.

The *lifetime* of a species is the time period during which its concentration would decrease to $1/e$, calculated on the basis of the actual rates of the processes and by

assuming that the investigated species is not produced. If species A is consumed in a single first-order reaction, then its concentration change can be calculated using Eq. (6.1). If at time τ_A we obtain that $k\tau_A = 1$, then $a(\tau_A) = a_0/e$, that is, the concentration of species A has decreased to $1/e$ of the initial value. This means that the lifetime of species A is $\tau_A = 1/k$. If a species is consumed in first-order reactions only, then the change in its concentration can be calculated from

$$a(t) = a_0 \exp\left(-t\sum_j k_j\right) \tag{6.9}$$

Therefore, the lifetime of A is the reciprocal of the sum of the rate coefficients: $\tau_A = 1/\sum_j k_j$. This, for example, is how the lifetime of an excited species is calculated in photochemical systems (see Pilling and Seakins (1995), p 279).

In the atmosphere, the concentrations of radicals are low; thus, the products of two radical concentrations are very small making the rates of radical−radical reactions also very small. For this reason, radical−radical reactions are usually not considered in atmospheric chemical mechanisms with the exception of peroxy−peroxy radical reactions. The rate coefficients of molecule−molecule reactions are also usually very small. Therefore, atmospheric chemical mechanisms (unlike, e.g. combustion mechanisms) usually do not contain reaction steps in which identical species react with each other (reaction type $2A \rightarrow B$). For this reason, in atmospheric chemistry, the production rates for most species can be calculated using the general equation:

$$dY_i/dt = P_i - L_i Y_i \tag{6.10}$$

where the production term P_i and the consumption term L_i do not depend on concentration Y_i, but may depend on the concentrations of all the other species. Therefore, in atmospheric chemistry, the usual definition (Hesstvedt et al. 1978) of the lifetime of species i is $\tau_i = 1/L_i$.

In a general kinetic reaction mechanism, there are second-order reactions, and there may also be reaction steps of the type $2A \rightarrow B$. Therefore, the definition given in Eq. (6.10) is not applicable. In the general case, the lifetime of species i can be calculated using the following equation:

$$\tau_i = -\frac{1}{J_{ii}} \tag{6.11}$$

where J_{ii} is the i-th element of the diagonal of the Jacobian (see Eq. (2.10)). A consequence of the structure of the kinetic system of differential equations and the rule of the derivation of the Jacobian is that element J_{ii} is usually negative for any concentration set, if species i has a consuming reaction. If this species does not have a consuming reaction, then element J_{ii} is zero. The corresponding element can be

positive only if the mechanism contains reactions of the type $\mathrm{X} \rightarrow 2\ \mathrm{X}$ or $2\ \mathrm{X} \rightarrow 3\ \mathrm{X}$. These represent lumped one-step autocatalytic reactions and would not therefore be present in comprehensive reaction schemes representing only elementary reactions. The lifetime defined by equation (6.11) is the generalisation of all previously introduced definitions. It can be calculated for any reaction mechanism, and is equivalent to photochemical and atmospheric chemical lifetimes (Turányi et al. 1993).

The previous statement will now be illustrated for two simple examples. As previously, the concentrations of a species will be denoted by small italic letters. The first mechanism to be investigated is the following:

$$\begin{array}{ll} \mathrm{A} \rightarrow \mathrm{B} & k_1 \\ \mathrm{A} \rightarrow \mathrm{C} & k_2 \end{array}$$

The change in concentration of species A over time is $a(t) = a_0 \exp(-(k_1 + k_2)\, t)$, and therefore, its lifetime is $\tau_\mathrm{A} = 1/(k_1 + k_2)$. Using atmospheric chemical notation,

$$\mathrm{d}a/\mathrm{d}t = P_\mathrm{A} - L_\mathrm{A}\, a = 0 - (k_1 + k_2)\, a \tag{6.12}$$

The atmospheric chemical lifetime is $\tau_\mathrm{A} = 1/L_\mathrm{A} = 1/(k_1 + k_2)$. The corresponding element of the Jacobian is

$$J_{\mathrm{AA}} = \frac{\partial(\mathrm{d}a/\mathrm{d}t)}{\partial a} = -(k_1 + k_2) \tag{6.13}$$

The lifetime calculated from the Jacobian is again $\tau_\mathrm{A} = -J_{\mathrm{AA}} = 1/(k_1 + k_2)$.

Let us consider now a mechanism in which species A is consumed in a second-order reaction:

$$\begin{array}{ll} \mathrm{A} \rightarrow \mathrm{B} & k_1 \\ \mathrm{A} + \mathrm{C} \rightarrow \mathrm{D} & k_2 \\ \mathrm{B} \rightarrow \mathrm{A} & k_3 \end{array}$$

Equation $\tau_\mathrm{A} = 1/\sum_j k_j$ for the calculation of the photochemical lifetime is not applicable here. Using atmospheric chemical notation, the production rate of species A is

$$\mathrm{d}a/\mathrm{d}t = P_\mathrm{A} - L_\mathrm{A}\, a = k_3\, b - (k_1 + k_2\, c)\, a \tag{6.14}$$

The calculated atmospheric chemical lifetime, $\tau_\mathrm{A} = 1/L_\mathrm{A} = 1/(k_1 + k_2\, c)$, depends on the actual concentration of species C. The corresponding element of the Jacobian is

$$J_{AA} = \frac{\partial(da/dt)}{\partial a} = -(k_1 + k_2\, c), \tag{6.15}$$

which results in lifetime $\tau_A = -1/J_{AA} = 1/(k_1 + k_2\, c)$.

The lifetime of a species can be used to predict what happens if the concentration of this species is changed suddenly. Such a sudden concentration change can be obtained, for example, if a precursor is added to the mixture and the precursor is decomposed by flash photolysis, inducing a sudden increase of the concentration of the photolysis products. This type of method becomes useful in the design of experiments aiming to determine rate coefficients for certain types of gas-phase reactions, and hence, an example will now be discussed.

Assume that in a given gas mixture, acetone and CO have low reactivity, whilst the radical CH_3 reacts very quickly with the species present in the gas mixture. Put a different way, CO has a long lifetime, whilst the lifetime of CH_3 is short. The system can be investigated by adding a small amount of acetone so that it does not perturb the system, and then, by using a laser flash of wavelength 193 nm, a part of the acetone can be suddenly decomposed. The duration of the laser flash would be a few nanoseconds (10^{-9} s), whilst the characteristic time of the concentration changes in the system is much longer. The chemical equation for the decomposition of acetone is

$$CH_3COCH_3 \rightarrow CO \; + \; 2\, CH_3$$

This means that the decomposition of acetone results in extra CO and CH_3. The concentration of CO is increased according to a step function, and since the consumption of CO is slow, this extra CO concentration remains in the system, i.e. the concentration of CO remains constant. However, the higher CH_3 concentration results in a higher consumption rate, and therefore, the concentration of CH_3 quickly returns near to the pre-perturbation value. As an example, acetone was photolysed in the presence of CCl_3Br in the gas mixture and the methyl radicals produced reacted rapidly with the CCl_3Br, whilst CO was a chemically inert species in this mixture (Macken and Sidebottom 1979).

The determination of the lifetime of radical species in the atmosphere has also been proposed as a method of exploring the discrepancies between atmospheric field measurements and model outputs. Historically, the concentration of the radical OH has been overpredicted by tropospheric models even when major hydrocarbon species concentrations are constrained in the model by relevant field measurements. Since OH is central to atmospheric oxidation processes, and itself governs the atmospheric lifetime of most anthropogenic and biogenic trace species, the correct prediction of its concentration is critical to tropospheric chemical modelling. The failure to predict its concentration correctly highlights uncertainties in the description of tropospheric chemical processes and possible missing reaction pathways that consume OH. Since the reactions contributing to the consumption of OH in the troposphere are first order in OH, the lifetime of OH is given by the expression $\tau_{OH} = 1/L_{OH} = 1/(\sum k_j\, c_i)$, where c_i is the concentration of a co-reactant

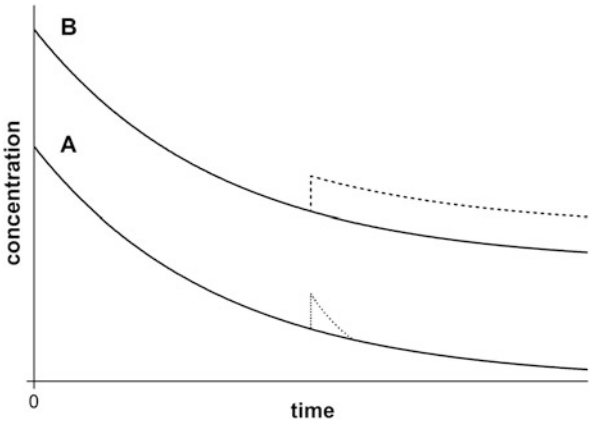

Fig. 6.1 Species A is a fast variable and following a rapid change in concentration, the perturbed concentration curve quickly approaches the original one. Species B is a slow variable; therefore, the distance between the original and the perturbed concentration−time curve remains almost constant in time

of OH and k_j is the bimolecular rate coefficient for the reaction between the co-reactant and OH (Bell et al. 2003). Measuring the lifetime of OH in the troposphere therefore gives an additional constraint in model/measurement comparison. In particular, it allows explicit recognition of situations where the full range of co-reactants has not been fully characterised, i.e. by comparing the modelled and measured lifetime of OH, one can determine the fraction of OH sinks that are not being measured in field experiments (Kovacs and Brune 2001). These types of measurements may also be used for model validation purposes. For this reason, field instruments which attempt to measure OH lifetime in the atmosphere using perturbation methods have been under development for several years, as well as being deployed in both semi-polluted and remote tropical locations (Lee et al. 2009; Ingham et al. 2009). Another development described in Mao et al. (2009) is the use of flash photolysis methods where OH is rapidly generated by photolysing water vapour with 185 nm UV light. The decay of OH in ambient air is then measured giving the first-order loss rate and hence OH reactivity. The study of Mao et al. was based in Hawaii and Alaska, and it attempted to explore the reactive transport of Asian pollution over the Pacific Ocean. The under prediction of OH reactivity by the chemical transport models was attributed to missing reactions of highly reactive volatile organic compounds (VOCs) that had HCHO as an oxidation product. OH lifetime studies over a US forest were also used to indicate the presence of unknown but reactive biogenic VOCs that were consuming OH (Di Carlo et al. 2004).

Within a chemical system, the long lifetime variables are called *slow variables*. For such variables, the distance between the original and the perturbed trajectories remains almost constant in time, whilst for the short lifetime, the so-called fast variables, the perturbed trajectory quickly approaches the original trajectory (see Fig. 6.1) (Klonowski 1983; Lee and Othmer 2010). It is important to note that there is no relationship between the magnitude of the production rate and the separation of slow and fast variables. This partition is based only on the rate of response to a perturbation. A high production rate (quickly changing concentration) may belong

to a slow variable, and an almost zero production rate (stationary concentration) may belong to a fast variable.

The implication of distinguishing between fast and slow variables is that a short time after the perturbation, the values of the fast variables are determined by the values of the slow ones. Appropriate algebraic expressions to determine the values of the fast variables as functions of the values of the slow ones can therefore be developed. This is the starting point of model reduction methods based on timescale analysis. One such method was introduced in Sect. 2.3 where the quasi-steady-state approximation (QSSA) was demonstrated for the reduction in the number of variables of a simple example. In this case, the system timescales were directly associated with chemical species. We shall see in the later discussion that this need not always be the case.

6.3 Application of Perturbation Theory to Chemical Kinetic Systems

For equation systems of low dimension, the investigation of the inherent timescales can be carried out through a non-dimensionalisation process. Small parameters can then often be identified indicating fast variables. A discussion of non-dimensionalisation procedures for a simplified 4-variable model describing the horseradish peroxidase reaction can be found in Chap. 12 of Scott (1990). The 4-variable model can be described by the following reaction steps:

$$
\begin{array}{lcll}
\mathrm{A}+\mathrm{B}+\mathrm{X} & \rightarrow & 2\mathrm{X} & k_1 \\
2\mathrm{X} & \rightarrow & 2\mathrm{Y} & k_2 \\
\mathrm{A}+\mathrm{B}+\mathrm{Y} & \rightarrow & 2\mathrm{X} & k_3 \\
\mathrm{X} & \rightarrow & \mathrm{P} & k_4 \\
\mathrm{Y} & \rightarrow & \mathrm{Q} & k_5 \\
\mathrm{X}_0 & \rightarrow & \mathrm{X} & k_6 \\
\mathrm{A}_0 & \leftrightarrows & \mathrm{A} & k_{7,}k_{-7} \\
\mathrm{B}_0 & \rightarrow & \mathrm{B} & k_8
\end{array}
$$

In dimensionless form, the rate equations can be written as

$$\mathrm{d}a/\mathrm{d}t = -abx - \gamma aby + p_2 - p_3 a \tag{6.16}$$

$$\mathrm{d}x/\mathrm{d}t = abx - 2x^2 + 2\gamma aby - x + p_1 \tag{6.17}$$

$$\mathrm{d}y/\mathrm{d}t = 2x^2 - \gamma aby - \alpha y \tag{6.18}$$

$$\mathrm{d}b/\mathrm{d}t = \varepsilon[-abx - \gamma aby + p_0] \tag{6.19}$$

where a, x, y, b are dimensionless concentrations and p_0, p_3, α, γ, ε are parameters involving the rate constants. The parameter ε is small relative to the other

parameters and indicates that b will evolve on a slower timescale than the other variables. The non-dimensionalisation procedure has therefore revealed a timescale separation in this system which suggests that the system can be decoupled into a "fast" 3-variable subset (a,x,y) and a slowly evolving variable b.

For larger systems such as those typically found in complex chemical problems, non-dimensionalisation may be impractical, and hence, numerical perturbation methods are generally used to investigate system dynamics and to explore timescale separation. By studying the evolution of a small disturbance or perturbation to the nonlinear system, it is possible to reduce the problem to a locally linear one. The resulting set of linear equations is easier to solve, and information can be obtained about the local timescales and stability of the nonlinear system. Several books on mathematics and physics (see e.g. Pontryagin 1962) discuss the linear stability analysis of the stationary states of a dynamical system. In this case, the dynamical system, described by an ODE, is in stationary state, i.e. the values of its variables are constant in time. If the stationary concentrations are perturbed, one of the possible results is that the stationary state is asymptotically stable, which means that the perturbed system always returns to the stationary state. Another possible outcome is that the stationary point is unstable. In this case, it is possible that the system returns to the stationary state after perturbation towards some special directions but may permanently deviate after a perturbation to other directions. A full discussion of stationary state analysis in chemical systems is given in Scott (1990).

In the following paragraphs, a more complicated system will be investigated, which is a generalisation of the stability analysis applied to stationary states. The system we investigate is described by the ODE defined in Eq. (2.9), i.e. it is an initial value problem where the concentrations are changing in time. We now ask the following question: how will the system respond, if one or several concentrations are changed instantaneously at any point in time? This type of analysis can be used to investigate inherent timescales within dynamical chemical systems, the couplings between species, and to determine species which drive the slow, intermediate and fast dynamics of the system (Tomlin et al. 2001).

Let us change the concentrations of several species during the course of the reaction at an arbitrarily selected time $t_0 = 0$ according to the vector $\Delta\mathbf{Y}^0$:

$$\widetilde{\mathbf{Y}}(0) = \mathbf{Y}(0) + \Delta\mathbf{Y}^0 \tag{6.20}$$

The vector of concentrations $\widetilde{\mathbf{Y}}(t)$ at a later time t can be given as the sum of the original concentrations $\mathbf{Y}(t)$ and the effect of the perturbation $\Delta\mathbf{Y}(t)$:

$$\widetilde{\mathbf{Y}}(t) = \mathbf{Y}(t) + \Delta\mathbf{Y}(t) \tag{6.21}$$

The time derivative of $\widetilde{\mathbf{Y}}(t)$ can be calculated in two ways. For the first method (a linearisation), a Taylor series expansion is used with higher-order terms neglected:

$$\frac{\mathrm{d}\widetilde{\mathbf{Y}}}{\mathrm{d}t} = \frac{\mathrm{d}(\mathbf{Y} + \Delta\mathbf{Y})}{\mathrm{d}t} \approx \mathbf{f}(\mathbf{Y}, \mathbf{p}) + \frac{\partial \mathbf{f}}{\partial \mathbf{Y}} \Delta\mathbf{Y} = \mathbf{f}(\mathbf{Y}, \mathbf{p}) + \mathbf{J}\,\Delta\mathbf{Y} \tag{6.22}$$

Alternatively, the derivative of the sum $\mathbf{Y} + \Delta\mathbf{Y}$ is calculated as the sum of the derivatives:

$$\frac{\mathrm{d}\widetilde{\mathbf{Y}}}{\mathrm{d}t} = \frac{\mathrm{d}(\mathbf{Y} + \Delta\mathbf{Y})}{\mathrm{d}t} = \mathbf{f}(\mathbf{Y}, \mathbf{p}) + \frac{\mathrm{d}\,\Delta\mathbf{Y}}{\mathrm{d}\,t} \tag{6.23}$$

The left-hand sides of Eqs. (6.22) and (6.23) are equal to each other, and therefore,

$$\frac{\mathrm{d}\Delta\mathbf{Y}}{\mathrm{d}t} = \mathbf{J}\ \ \Delta\mathbf{Y} \tag{6.24}$$

During very short time periods, the Jacobian does not change significantly (the Jacobian $\mathbf{J}_0 = \mathbf{J}(t_0)$ is constant), and therefore, the differential equation (6.24) can be solved analytically:

$$\Delta\,\mathbf{Y}(t) = e^{\mathbf{J}_0 t}\ \ \Delta\mathbf{Y}^0 \tag{6.25}$$

giving the change in concentration at time t due to the perturbation at time t_0. We are used to meeting exponential functions with scalar arguments in science, whereas here $\mathbf{J_0}$ is a matrix. However, an exponential function can be defined as a series of power functions. Since the product and sum of matrices can be interpreted, the series of power functions can also be interpreted for matrices. This series will be convergent for any matrix, and therefore, the exponential function may have a matrix argument.

The first step in the calculation of the matrix exponential can be (Prasolov 1994) the decomposition of matrix $\mathbf{J}_0$ to its Jordan canonical form $\boldsymbol{J}$ using the invertible matrix $\mathbf{P}$:

$$\mathbf{J}_0 = \mathbf{P}\boldsymbol{J}\mathbf{P}^{-1} \tag{6.26}$$

where

$$e^{\mathbf{J}_0 t} = \mathbf{P}e^{\boldsymbol{J}t}\mathbf{P}^{-1} \tag{6.27}$$

The eigenvalue−eigenvector decomposition of matrix $\mathbf{J}_0$ is the following:

$$\mathbf{J}_0 = \mathbf{V}\boldsymbol{\Lambda}\mathbf{W} \tag{6.28}$$

where matrix $\boldsymbol{\Lambda}$ is the diagonal matrix of eigenvalues ($\boldsymbol{\Lambda} = \mathrm{diag}(\lambda_1, \ldots, \lambda_n)$), matrix $\mathbf{V}$ contains the right eigenvectors as column vectors ($\mathbf{V} = [\,\mathbf{v}_1 \quad \ldots \quad \mathbf{v}_n\,]$) and matrix $\mathbf{W} = \mathbf{V}^{-1}$ contains the left eigenvectors as row vectors ($\mathbf{W} = [\,\mathbf{w}_1 \quad \ldots \quad \mathbf{w}_n\,]^T$).

The recent trend is that very large reaction mechanisms are created either manually or automatically for the combustion or the atmospheric decomposition of large organic molecules [see e.g. (Herbinet et al. 2010; Westbrook et al. 2011)], as discussed in Sect. 3.1. In such mechanisms, only a minority of the reaction steps has an experimentally measured rate coefficient, and most of the reaction parameters are estimated using simple rules. Therefore, it is common that many rate coefficients are identical within such mechanisms. A numerical consequence can be that an eigenvalue – eigenvector decomposition of the Jacobian does not exist. However, even in this case, the effect of concentration perturbations can always be studied on the basis of the Jordan decomposition of the Jacobian (Nagy and Turányi 2009), as discussed below.

The eigenvalues of a matrix may have algebraic and may have geometric multiplicity (Prasolov 1994). The algebraic multiplicity $a(\lambda)$ of eigenvalue λ is equal to the multiplicity of root λ of the characteristic polynomial. The geometric multiplicity $g(\lambda)$ is equal to the dimension of the eigensubspace belonging to λ, i.e. equal to the number of linearly independent eigenvectors belonging to eigenvalue λ. An eigenvalue is called degenerate if $g(\lambda) < a(\lambda)$. If at least one eigenvalue of matrix $\mathbf{J}_0$ is degenerate, then matrix $\mathbf{J}_0$ does not have an eigenvalue−eigenvector decomposition corresponding to Eq. (6.28). However, in all cases, the Jacobian $\mathbf{J}_0$ has a Jordan decomposition according to Eq. (6.26) (Nagy and Turányi 2009b).

If the Jacobian can be diagonalised according to Eq. (6.28), much simpler equations are obtained:

$$\Delta\mathbf{Y}(t) = e^{\mathbf{J}_0 t}\Delta\mathbf{Y}^0 = \sum_{l=1}^{n} e^{\lambda_l t}\mathbf{v}_l\left(\mathbf{w}_l\Delta\mathbf{Y}^0\right) = \sum_{l=1}^{n} e^{\lambda_l t}(\mathbf{v}_l \circ \mathbf{w}_l)\Delta\mathbf{Y}^0$$

$$= \sum_{l=1}^{n} e^{\lambda_l t}\mathbf{P}_l\Delta\mathbf{Y}^0 \tag{6.29}$$

where $\mathbf{v}_l$ is the l-th column of the right eigenvector matrix and $\mathbf{w}_l$ is the l-th row of the left eigenvector matrix. The projector matrix $\mathbf{P}_l$ can be calculated by the tensor product (also called dyadic product or outer product) of vectors $\mathbf{v}_l$ and $\mathbf{w}_l$.

The Jacobian is not a symmetric matrix, and therefore the eigenvalues can also be complex numbers. Let us assume now that the eigenvalues have zero imaginary components. Rewriting Eq. (6.29) to a form containing scalar valued functions only, the concentration changes can be described by the sum of exponential functions, where the arguments of the exponential functions contain the eigenvalues of the Jacobian. The number of eigenvalues is equal to the number of variables, and each eigenvalue is associated with a different timescale of the locally linear solution to the full equations. The eigenvalue with the largest negative real part corresponds to a perturbation which decays very quickly and is therefore associated with the fastest timescale. However, there is no one-to-one equivalence between the eigenvalues and the variables (concentrations of species). For nonlinear systems with species coupling, several different timescales may

contribute to the decay or growth of each species perturbation, and conversely several different species may contribute to each timescale. The calculation of eigenvectors is useful since the off-diagonal terms tell us about the couplings between species and the contributions of individual species to different timescale modes (see discussion below). In the general case, however, there is not necessarily a direct connection between the rate of return after the perturbation and the lifetime of an individual species defined by Eq. (6.11) as highlighted in the following discussion.

If the concentration of a single species is changed by Δy_i^0 so that the perturbation is small enough to induce a linear response (which means that the rate of return is proportional to the extent of deviation), and so that the change in concentration of the other species is negligible, then the return of the perturbed concentration can be described by the following exponential function:

$$\Delta y_i(t) = \Delta y_i^0 \, e^{J_{ii} t} \tag{6.30}$$

If the perturbed species has a short lifetime (i.e. has a high reactivity), and there is sufficient separation between the timescales, then the conditions above are usually fulfilled. The concentrations of these species quickly return to the original trajectory, and the return can be described by a single exponential function. In this case, the exponent of the exponential is related [see Eq. (6.11)] to the lifetime of the species.

If the concentrations of several species are perturbed simultaneously, it is still possible that the return to the original trajectory is described by single exponential function, if the direction of the perturbation is appropriate. According to the diagonalisation of the Jacobian,

$$\mathbf{\Lambda} = \mathbf{W}\,\mathbf{J}_0\,\mathbf{V} \tag{6.31}$$

where $\mathbf{W}$ is the matrix of left eigenvectors (row vectors) and $\mathbf{V}$ is the matrix of right eigenvectors (column vectors). This equation is equivalent to the previous Eq. (6.28), since

$$\mathbf{WV} = \mathbf{VW} = \mathbf{I} \tag{6.32}$$

and thus

$$\mathbf{J}_0 = \mathbf{V\Lambda W} \tag{6.33}$$

where $\mathbf{I}$ is the identity matrix.

If the values of variables are changed by $\Delta \mathbf{Y}_j^0 = \alpha\,\mathbf{v}_j$, where α is a small scalar and $\mathbf{v}_j$ is the j-th column of matrix $\mathbf{V}$ (j-th right eigenvector), then using Eq. (6.29), the displacement of the values of variables from the original values as a function of time can be calculated using the following equation:

$$\Delta \mathbf{Y}_j(t) = \Delta \mathbf{Y}_j^0 e^{\lambda_j t} \tag{6.34}$$

This means that, according to a local linear approximation, the approach from perturbation direction $\mathbf{v}_j$ to the original trajectory can be characterised by a single exponential function having parameter λ_j. The problem is that the Jacobian is not symmetrical, and therefore, λ_j can be a complex number.

If λ_j is a real number ($\mathrm{Im}(\lambda_j) = 0$), then in the space of concentrations, the point characterising the actual state of the system is moving along the original trajectory, and its distance from the trajectory is changing in time according to a real exponential function. If λ_j is a real number (i.e. if $\lambda_j = \mathrm{Re}(\lambda_j)$), then the distance of the perturbed system from the unperturbed one is exponentially decreasing ($\lambda_j < 0$), is increasing ($\lambda_j > 0$) or remains constant ($\lambda_j = 0$).

If λ_j is a complex number ($\mathrm{Im}(\lambda_j) \neq 0$), then the point is moving in a 2D subspace defined by the real and imaginary parts of the complex eigenvector. This point is moving with rotational frequency $\omega = \mathrm{Im}(\lambda_j)$ (i.e. with period $2\pi/\mathrm{Im}\ (\lambda_j)$) in an ellipse having axes with length $\exp(\mathrm{Re}(\lambda_j)\, t)$. In the general case, the point of the system follows an elliptic spiral along the trajectory of the original (unperturbed) system. If λ_j is a complex number and its real part ($\mathrm{Re}(\lambda_j)$) is negative, then the average distance (i.e. average over a period) is decreasing with time. The approach is faster, if $\mathrm{Re}(\lambda_j)$ is a lower negative number, i.e. if $|\,\mathrm{Re}(\lambda_j)\,|$ is larger and $\mathrm{Re}(\lambda_j)$ is negative. If $\mathrm{Re}(\lambda_j)$ is zero, then the distance averaged over a period is constant. If Re (λ_j) is positive, then the average distance between the original and the perturbed states is increasing and the increase is faster if $\mathrm{Re}(\lambda_j)$ is larger. The ratio $1/|\mathrm{Re}(\lambda_j)|$ is called the *j*-th timescale of the dynamical system.

The dynamic behaviour of the system tends to be dominated by the motion associated with either the positive eigenvalues or the smallest negative ones, since those with large negative eigenvalues tend to relax to their local equilibria very quickly and therefore do not influence the slower modes.

If a small amount of a species is added to a reacting mixture, the resulting higher concentration may increase the rate of the consuming reactions. Consequently, the difference between the old and new concentration trajectory diminishes. This case is associated with the presence of negative eigenvalues. If the behaviour of the system is controlled by an autocatalytic species, then adding the autocatalyst induces changes that further increase the concentration of the autocatalyst. A similar behaviour is found when the added species can be converted quickly to the autocatalyst. In such systems, the Jacobian has at least one positive $\mathrm{Re}(\lambda_j)$. For example, in explosions, the highest eigenvalue of the Jacobian is positive during rapid changes of the concentrations, whilst the real parts of all eigenvalues are negative before and after this period.

A systematic investigation of explosions based on the eigenanalysis of the Jacobian is called *chemical explosive mode analysis* (CEMA) (Lu et al. 2010; Luo et al. 2012c). An explosion index is defined for the explosive modes, which is similar to the radical pointer of the CSP method discussed below. This indicates

the contribution of the various species and temperature to the explosion process and thus facilitates the distinction between radical and thermal runaways.

It is clear that, based on small perturbations of concentrations, lifetimes can be related to chemical kinetic systems. These lifetimes do not belong to species, however, but to combinations of species concentrations defined by the left eigenvectors of the Jacobian, called *modes*. A matrix Jacobian of size $N_S \times N_S$ has N_S eigenvalues, and therefore, the number of modes is identical to the number of variables. In the case of a linear system (in reaction kinetics, this means that the mechanism consists of first-order and zeroth-order reactions only), the Jacobian is constant and does not depend on the values of variables (concentrations). If the system is nonlinear, which is the case for most reaction kinetic systems, the Jacobian depends on the values of variables, i.e. the timescales depend on the concentrations. In other words, the set of timescales belong to a given point in the space of concentrations (phase space) and are different from location to location (or from time point to time point if the concentrations change in time).

As Eq. (6.34) shows, concentration perturbations along the directions of the right eigenvectors of the Jacobian have special importance. Therefore, it is justified to introduce a new coordinate system. It is called the space of modes, and its axes are defined by the eigenvectors. Using the left eigenvectors of the Jacobian, a concentration set (point in the space of concentrations) can always be converted to a point in the space of modes. The vector of modes $\mathbf{z}$ can be calculated using the following equation:

$$\mathbf{z} = \mathbf{W}\ \mathbf{Y} \tag{6.35}$$

The i-th mode coordinate is

$$z_i = \mathbf{w}_i\ \mathbf{Y} \tag{6.36}$$

Knowing the vector of modes, the concentration vector (or concentration y_i) can be calculated:

$$\mathbf{Y} = \mathbf{V}\ \mathbf{z} \tag{6.37}$$

$$y_i = \mathbf{v}_i\ \mathbf{z} \tag{6.38}$$

The initial value problem (2.9) has been used for the calculation of concentration changes in time. A similar initial value problem can be used to calculate the change of modes $\mathbf{z}$ in time:

$$\frac{\mathrm{d}\mathbf{z}}{\mathrm{d}t} = \mathbf{W}\ \mathbf{f}(\mathbf{V}\mathbf{z}), \qquad \mathbf{z}_0 = \mathbf{W}\ \mathbf{Y}_0 \tag{6.39}$$

Since the Jacobian depends on the concentrations for nonlinear chemical kinetic equations, the transformations above are also different at different points in the concentration space.

Let us now follow the consequence of an arbitrary perturbation $\Delta\mathbf{Y}$ in the space of modes. A concentration perturbation $\Delta\mathbf{Y}$ can be transformed to a mode perturbation $\Delta\mathbf{z}$ in the following way:

$$\Delta\mathbf{z} = \mathbf{W}\,\Delta\mathbf{Y} \tag{6.40}$$

Using a linear approximation, the change of $\Delta\mathbf{Y}$ in time can be obtained by solving the following ODE:

$$\frac{\mathrm{d}\Delta\mathbf{Y}}{\mathrm{d}t} = \mathbf{J}_0\,\Delta\mathbf{Y} \tag{6.41}$$

The equation is then extended by unit matrix $\mathbf{VW} = \mathbf{I}$, and both sides are multiplied by matrix $\mathbf{W}$:

$$\mathbf{W}\frac{\mathrm{d}\Delta\mathbf{Y}}{\mathrm{d}t} = \mathbf{W}\mathbf{J}_0\mathbf{V}\mathbf{W}\,\Delta\mathbf{Y} \tag{6.42}$$

Using eqs. (6.40) and (6.31), the equation above can be rewritten as

$$\frac{\mathrm{d}\Delta\mathbf{z}}{\mathrm{d}t} = \mathbf{\Lambda}\,\Delta\mathbf{z} \tag{6.43}$$

Since matrix $\mathbf{\Lambda}$ is diagonal, for each mode coordinate, we obtain that

$$\frac{\mathrm{d}\Delta z_i}{\mathrm{d}t} = \lambda_i\,\Delta z_i \tag{6.44}$$

If the initial (belonging to time $t = 0$) perturbation is $\Delta\mathbf{z}^0 = \mathbf{W}\,\Delta\mathbf{Y}^0$, then

$$\Delta z_i(t) = \Delta z_i^0 e^{\lambda_i t} \tag{6.45}$$

This means that in the space of modes, perturbations of the mode coordinates respond independently of each other. What this means physically is that the transformation matrix $\mathbf{W}$ shows us how each species contributes to the modes associated with each eigenvalue. By ordering the eigenvalues, we can see which species are associated with the slow and fast modes of the system. This can allow us to identify species contributing to the fast-decaying modes which locally equilibrate (i.e. approximately return to their unperturbed values) and those which contribute to the slower modes which may dominate the longer-term dynamics of the model.

This type of approach was used in the study of mechanisms describing tropospheric chemistry by Tomlin et al. (2001). A simple mechanism describing CO oxidation and the interaction between ozone and nitrogen species is first used as an illustrative example. Figure 6.2 illustrates the relationship between timescale modes and species for this simple system as determined by the left eigenvectors. In the figure, mode 1 is the fastest mode ($\lambda \approx -8 \times 10^8$) and can be seen to be

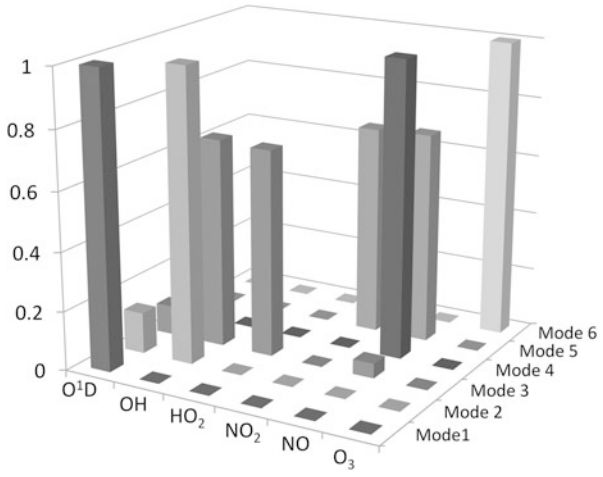

Fig. 6.2 A schematic diagram showing the relative relationships between species and modes for a simple six-variable tropospheric model, adapted from Tomlin et al. (2001)

associated almost exclusively with the species O^1D which has an extremely short lifetime. The second mode ($\lambda \approx -70$) is mainly dominated by OH, but the third mode ($\lambda \approx -8$) contains contributions from both OH and HO_2. The corresponding 3×3 submatrix is block triangular, and whilst the radical species are coupled to each other, they do not couple back to the major species which implies that the fastest timescales could be separated from the slow modes. For a more complex tropospheric butane oxidation scheme, the study showed that the intermediate (i.e. slow but not conserved) modes were dominated by the species NO_2, HONO, NO_3, HNO_3, PAN ($CH_3CO_3NO_2$) and by several carbonyl species for most of the diurnal cycle under high background NOx conditions. These are the species, therefore, which drive the important dynamics of the system. Since the timescale analysis was performed at many time points throughout the simulations, it was also able to highlight that ozone joined this group only at dawn and dusk when photolysis-driven reaction rates change rapidly.

Reaction mode analysis was also used for the investigation of time hierarchies of a biochemical kinetic mechanism that describes the carbohydrate uptake and metabolism of bacterium *Escherichia coli* (Kremling et al. 2004). The Jacobian was calculated at the steady-state point of the system, and the analysis revealed which reaction steps contribute mainly to the reaction modes having different timescales.

6.4 Computational Singular Perturbation Theory

Lam and Goussis elaborated a detailed theory based on the application of computational perturbation methods for the investigation of reaction mechanisms. This family of methods is called *computational singular perturbation* theory and is often

abbreviated as *CSP*. In a similar way to that described in Sect. 6.3, CSP uses variable transformations in order to separate the timescales of complex chemical models. It was originally designed to enable a user to investigate the presence of partial equilibrium (Sect. 2.3.2) and quasi-steady-state (Sect. 2.3.4) relationships within a complex kinetic mechanism without the need for specialist chemical intuition or expertise by providing appropriate numerical measures. The CSP theory is summarised below in accordance with the recent article of Kourdis and Goussis (Kourdis and Goussis 2013).

If the Jacobian of the kinetic system of differential equations has M eigenvalues with negative real parts that are much larger (i.e. more negative) than the other Re (λ_j) values, then the solution is quickly attracted onto an $(N_s–M)$-dimensional surface Ω, which is called the slow invariant manifold (SIM) (Fenichel 1979). Denote $T_Y\Omega$ and T_YF as two subspaces, where the slow subspace $T_Y\Omega$ is the space of movement on Ω and the fast subspace T_YF contains the directions of fast approaches to the manifold. These spaces can be spanned by the following basis vectors: $T_YF = \text{span}(\mathbf{a}_i, i = 1, \ldots, M)$ and $T_Y\Omega = \text{span}(\mathbf{a}_i, i = M + 1, \ldots, N_s)$. Vectors $\mathbf{a}_i$ form matrices $\mathbf{A}_r = [\mathbf{a}_1, \mathbf{a}_2, \ldots, \mathbf{a}_M]$ and $\mathbf{A}_s = [\mathbf{a}_{M+1}, \mathbf{a}_{M+2}, \ldots, \mathbf{a}_{Ns}]$. On this basis, the right-hand side of the kinetic ODE can be decomposed as

$$\mathbf{f} = \mathbf{f}_{\text{fast}} + \mathbf{f}_{\text{slow}} \tag{6.46}$$

Here $\mathbf{f}_{\text{fast}} = \mathbf{A}_r\mathbf{z}^r$ and $\mathbf{f}_{\text{slow}} = \mathbf{A}_s\mathbf{z}^s$, and the corresponding amplitudes are defined as $\mathbf{z}^r = \mathbf{B}^r\mathbf{f}$ and $\mathbf{z}^s = \mathbf{B}^s\mathbf{f}$. Vectors $\mathbf{b}^i$ are defined by $\mathbf{b}^i\mathbf{a}_j = \delta^i_j$.

When the trajectory reaches the SIM, the fast timescales become exhausted; vector $\mathbf{f}$ has no component in the fast subspace T_YF, and it is entirely in the slow subspace $T_Y\Omega$. These exhausted timescales are termed "dead" or "exhausted" modes. Once the fast timescales have become exhausted, the solution evolves along the SIM according to the slow timescales (or "active" modes). This state of the system is governed by relations $\mathbf{z}^r \approx \mathbf{0}$ and $\mathrm{d}\mathbf{Y}/\mathrm{d}t \approx \mathbf{f}_{\text{slow}}$. In the CSP methodology, an iterative method is used to calculate the vectors that span subspaces T_YF and $T_Y\Omega$, using the so-called $\mathbf{b}^r$ and $\mathbf{a}_r$-refinements (Lam and Goussis 1988, 1991; Zagaris et al. 2004; Valorani et al. 2005b).

In the CSP method, the equation system, $\mathbf{z}^r \approx \mathbf{0}$ represents conservation relations which could be generalisations of QSSA and partial equilibrium assumptions. Dormant modes may also exist which have close to zero amplitude for some periods of the simulation, which may grow at a later time. Conserved modes may also be present due to element conservation, as discussed in Sect. 2.3.5. Discarding the dead modes, or replacing them with conservation relations, results in a less stiff system of equations which could potentially lead to computational savings. However, if the vectors $\mathbf{a}_r$ have to be determined numerically, then any savings provided by reducing stiffness may be outweighed by the cost of determining the new basis sets at each time point. In reality, CSP has been mainly used for the investigation of system dynamics and within the context of mechanism reduction. Applications of the CSP method in the context of mechanism reduction will be discussed in Sects. 7.2.1 and 7.9.

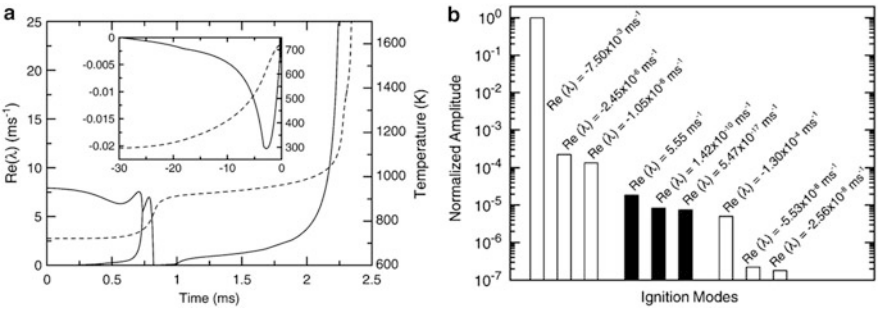

Fig. 6.3 An example of large amplitude CSP modes obtained from a modelling study of dimethyl ether auto-ignition in a rapid compression machine (Mittal et al. 2008) for a DME/O_2/N_2 mixture (1/4/30 molar composition) initially at 523 Torr and 297 K ($P_c = 20.1$ bar, $T_c = 720$ K). (**a**) Temperature (*dashed lines*) and the highest eigenvalue (*solid lines*) during the time evolution to ignition (*insert* shows results during compression stroke). (**b**) Spectrum at 0.5 ms before the end of the compression stroke. *Open bars* correspond to decaying or exhausted modes (negative eigenvalues), *solid bars* to explosive modes (positive eigenvalues). Reproduced from Mittal et al. (2008) with permission from Elsevier

The number of conserved, dormant, exhausted and active modes can be identified using CSP along a system trajectory (or in space, e.g. in a stationary flame). The number of active modes indicates the number of variables required to accurately represent the system dynamics. For systems proceeding towards a steady-state, starting from an arbitrary concentration set, the active modes should become exhausted one after the other. However, during ignition in combustion systems, for example, positive modes may temporarily grow as illustrated in Fig. 6.3 for the ignition of dimethyl ether in a rapid compression machine (Mittal et al. 2008).

The first article about the CSP method was published in 1988 (Lam and Goussis 1988), and up until 1994, four further articles (Lam and Goussis 1991, 1994; Goussis and Lam 1992; Lam 1993) were published by Lam and Goussis. Further additions to the theory were published by Lam (2006, 2013), whilst Goussis and his co-workers also published many extensions (Goussis 1996; Hadjinicolaou and Goussis 1998; Goussis et al. 2003; Valorani et al. 2006) and applications of CSP in the fields of combustion (Massias et al. 1999a, b; Valorani and Goussis 2001; Valorani et al. 2003, 2005a, b, 2006, 2007; Goussis and Skevis 2005; Goussis et al. 2005a; Lee et al. 2005, 2007; Prager et al. 2009), atmospheric chemistry (Neophytou et al. 2004) and systems biology (Goussis and Najm 2006; Kourdis et al. 2010; Kourdis and Goussis 2013). Several other researchers also contributed to the development of the CSP theory (Lu et al. 2001; Zagaris et al. 2004; Adrover et al. 2006). The method has also been widely utilised by others for the investigation and reduction of atmospheric models (Løvås et al. 2006; Mora-Ramirez and Velasco 2011) and in combustion [e.g. Treviño (1991), Treviño and Solorio (1991), Treviño and Mendez (1991), 1992), García-Ybarra and Treviño (1994), Treviño and Liñan (1995), Fotache et al. (1997), Løvås et al. (2002), Mittal et al. (2008), Lu and Law (2008a, b), Gupta et al. (2011)].

6.5 Slow Manifolds in the Space of Variables

Roussel and Fraser (1991) also carried out timescale analysis of reaction kinetic systems. Their approach was to make a comprehensive investigation of the features of trajectories in the concentration phase space starting from many different initial conditions using examples of small enzyme kinetic systems, i.e. it was a geometric-based analysis. They demonstrated that the progress of a reaction can be interpreted as the point defining the state of the system always moving along certain multidimensional surfaces, with the dimension of these surfaces being smaller than the full dimension of the concentration space.

In a closed system, if the simulation is started from an arbitrary point in concentration space, it will finally end up at the equilibrium point, whilst the values of conserved variables remain constant. The equilibrium point is determined by the conserved properties, which are defined by the initial state of the system. If in an isothermal system there are N_S species and N_C conserved properties, then the trajectory of the system will move on a hypersurface with dimension $N_S - N_C$. As time elapses, active modes will collapse, with the fastest mode relating to the largest negative eigenvalue relaxing first. The trajectory then approaches a hypersurface with dimension $N_S - N_C - 1$. The relaxation will be approximately according to an exponential function as it nears the surface (see Sect. 6.3). Trajectories may start from different initial points, but eventually approach this surface exponentially, although they never reach it exactly. The geometric object defined in this way is called a *slow manifold*. The word "slow" refers to the fact that the movement along the manifold is much slower than the approach to the manifold from a point that is far from it. This implies a timescale separation between the fastest mode and the other modes. In the following, we make the assumption that the surface corresponding to the manifold is reached exactly in order to simplify the discussion and will return to an estimation of errors later in this section.

When the second fastest mode relaxes, the trajectory will reach a surface with dimension $N_S - N_C - 2$. In a closed system, this process continues until the trajectory in the space of concentrations reaches a 3D surface, a 2D surface (a curved plane) and a 1D "surface" (a curved line) and finally ends up near the 0D equilibrium point. Therefore, following the ideas of Roussel and Fraser, we can imagine the system collapsing onto a cascade of manifolds of decreasing dimension with the fastest modes collapsing first and the slowest last. For a non-isothermal system, temperature may also be a variable increasing the dimension of the phase space by 1, but the same principles apply. In our discussions, we denote N_s as the dimension of the full system which may include temperature as a variable.

Figure 6.4 shows trajectories approaching a 1D manifold for an example based on simulations of a steady, one-dimensional premixed H_2/O_2 flame (Davis and Tomlin 2008b), where the different trajectories represent different flame conditions but all with the same asymptote. The figure shows a projection for a 2D plane where the axes represent the mass fraction of the oxygen radical and temperature T.

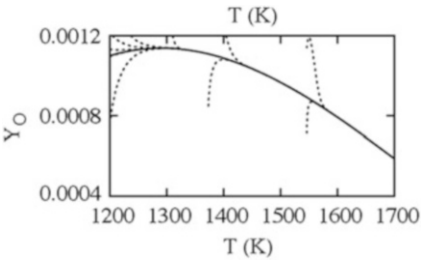

Fig. 6.4 An example of trajectories (*dotted curves*) approaching a 1D manifold (*solid curve*) for a steady, one-dimensional premixed H_2/O_2 flame. The figure shows a projection of the trajectories to the space of oxygen radical mass fraction Y_O and temperature T. Reprinted with permission from Davis and Tomlin (2008b). Copyright (2008) American Chemical Society

The trajectories are seen to be attracted to the manifold from all initial conditions although the approach is steeper from some directions.

From the figure, it appears that the trajectories reach exactly the same manifold, but it is easy to illustrate that a trajectory always only approaches the low-dimensional surface (or even the equilibrium point), but never reaches it exactly. In principle, time is reversible in a system defined by the system of ODEs (2.9). This means that calculating the trajectory from t_0 to t_1, and then continuing the simulation backwards in time from t_1 to t_0, the same concentration set should be recovered. This is impossible if trajectories starting from different initial conditions end up at exactly the same point. However, for most applications, the approximate nature of the slow manifolds is not a barrier to their use in model reduction strategies, since where large separations between timescales exist, the error related to the approximation of the slow manifold should be small.

In applicable situations, apart from the modes belonging to conserved properties (zero eigenvalues), the modes can be sorted to into fast or slow categories. If there are two slow modes, then, after some time, the trajectory will move along a 2D surface. This means that the change of all concentrations can be described by a two-variable system of differential equations, even if the values of all concentrations (and maybe also temperature) are changing in time. The concentrations of all other species would be determined by algebraic relationships relating them to the slow variables. Remember, however, as we discussed in Sect. 6.3, that these slow variables are not necessarily equivalent to specific species concentrations.

Maas and Pope developed an approach for the calculation of slow manifolds (Maas and Pope 1992a, b, 1994; Maas 1995, 1998, 1999; Maas and Thévenin 1998) utilising the approach of Roussel and Fraser, as well as the suggestion of Lam and Goussis, that timescales should be investigated pointwise via the eigenvalue−eigenvector decomposition of the Jacobian. Their approach was to tabulate these low-dimensional slow manifolds in phase space for several reaction systems in combustion. They called the slow manifolds *intrinsic low-dimensional manifolds* (*ILDM*).

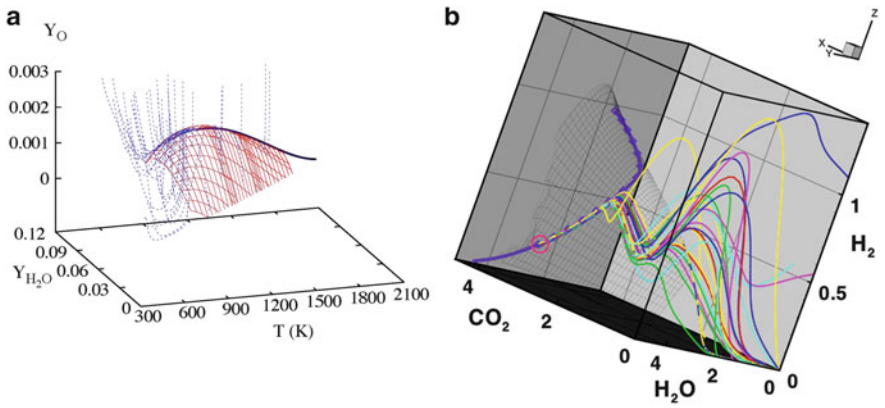

Fig. 6.5 (**a**) 2D and 1D manifolds for the hydrogen flame example. Starting from any point in phase space, the trajectories (*dotted lines*) quickly approach the 2D manifold (mesh surface) and then the 1D manifold (*bold line*) and move along it towards the equilibrium point. Reprinted with permission from Davis and Tomlin (2008b). Copyright (2008) American Chemical Society. (**b**) The collapse of reaction trajectories onto a 2D intrinsic low-dimensional manifold or ILDM (*black mesh*) for an *iso*-octane−air system plotted in a projection of the state space into $CO_2-H_2O-H_2$ concentration coordinates. 1D ILDM (*purple symbols*), 0D ILDM (equilibrium, *red circle*). The *coloured lines* are homogeneous reactor calculations for different fuels. Reprinted from (Blasenbrey and Maas 2000) with permission from Elsevier

Recently, Nicolini et al. (2013a, b) suggested a new approach for the calculation of low-dimensional slow manifolds in chemical kinetic systems. They transformed the original system of polynomial differential equations, which describes the chemical evolution, into a universal quadratic format. A region of "attractiveness" was found in the phase space, and a state-dependent rate function was defined that describes the evolution of the system.

The use of the low-dimensional manifold methods in the context of model reduction is discussed more fully in Sect. 7.10. However, an important question to arise in this section on timescale analysis is how we can determine for a given system what the appropriate dimension for the slow manifold should be. As the stationary point or equilibrium is approached, a 1D manifold may appropriately describe the dynamics of the system. However, we may be interested in dynamic behaviour far away from the stationary or equilibrium point where a 1D manifold is not appropriate. Clearly, in Fig. 6.5a, the behaviour at low temperatures in a steady H_2/O_2 flame is not 1D since the trajectories first approach the 2D manifold and move more slowly along it towards the 1D curve. Similar behaviour is presented in Fig. 6.5b where simulations of fuel oxidation in a homogeneous reactor are shown for a range of starting fuels. The trajectories converge onto the 2D manifold shown by the mesh and eventually reach the same equilibrium point. Making a priori estimates of the manifold dimension which is appropriate to represent the important dynamics of the system is not easy. One method might be to calculate low-dimensional manifolds of different dimensions and then compare the

behaviour of the system on these manifolds to trajectories calculated from the full model. This could be time consuming, however, and hence, approaches have been developed which attempt to estimate the dimension of the manifold along trajectories based on the analysis of timescale modes. The method of Tomlin et al. (2001) is based on ordering the eigenvalues for each of the timescale modes and investigating their collapse onto an (N_s-1)-dimensional manifold in an N_s-dimensional phase space. The dimension calculated this way is in good agreement with the results of alternative methods for the determination of dynamical dimension (Büki et al. 2002; Zsély et al. 2005). Valorani et al. (see Eq. (8) in Valorani et al. (2006)) derived a similar equation based on a CSP reasoning.

A consequence of Eqs. (6.25) and (6.44) is that the change of mode i after a perturbation can be described by the following equation:

$$\frac{\mathrm{d}z_i}{\mathrm{d}t} = \mathbf{w}_i\mathbf{f} = \mathbf{w}_i\mathbf{f}(\mathbf{Y}^m) + \mathbf{w}_i\frac{\mathrm{d}\,\Delta\mathbf{Y}}{\mathrm{d}t} = \frac{\mathrm{d}\Delta z_i}{\mathrm{d}t} \tag{6.47}$$

where $\mathbf{w}_i\mathbf{f}(\mathbf{Y}^m) = 0$, if point $\mathbf{Y}^m$ is on the "surface" of the manifold, since the direction of the movement $\mathbf{f}$ is always perpendicular to the surface spanned by the vectors $\mathbf{w}_i$. Here Δz_i denotes the size of perturbation along mode i and therefore gives a measure of the distance of the mode from its associated slow manifold.

By comparing Eqs. (6.44) and (6.47), we get

$$\mathbf{w}_i\mathbf{f} = \lambda_i\Delta z_i \tag{6.48}$$

The distance of the system from the slow manifold towards direction i can therefore be calculated from

$$\Delta z_i = \mathbf{w}_i\mathbf{f}/\lambda_i \tag{6.49}$$

This gives only the relative distance since the choice of eigenvectors is not unique and will affect the absolute value. By normalising we can obtain a measure of the relative distance of each mode from its equivalent slow manifold:

$$\Delta\widetilde{z}_i = \mathbf{w}_i\mathbf{f}/\lambda_i\frac{1}{\kappa + |\mathbf{w}_i\mathbf{Y}|} \tag{6.50}$$

where κ is a small parameter added to avoid division by zero. This calculated $\Delta\widetilde{z}_i$ distance is not expected to become exactly zero since the trajectory only approaches the manifold and can never be exactly on the corresponding surface. However, we can define a threshold z_{th} and state that the actual point has relaxed to the slow manifold if $\left|\Delta\widetilde{z}_i\right| < z_{\mathrm{th}}$. By estimating the distance of the system according to the fastest mode from the corresponding N_s-1-dimensional manifold and comparing it against a tolerance parameter, we can determine at each time point along a trajectory if the fastest mode has effectively been collapsed. It also follows that once the fastest mode has collapsed, then the error of assuming an

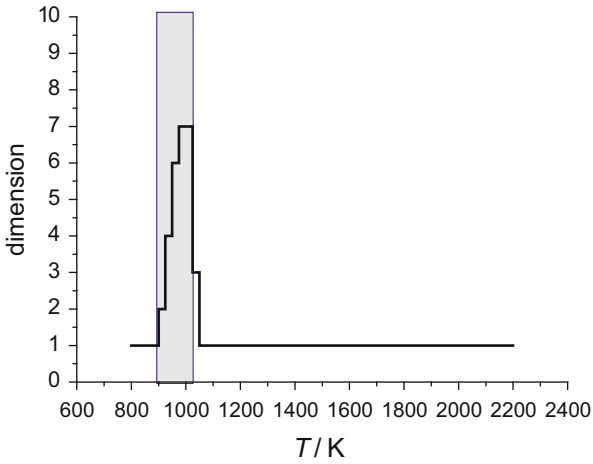

Fig. 6.6 The change of dimension during the adiabatic explosion of a stoichiometric hydrogen−air mixture. Due to the autocatalytic process, the dimension increases up to seven and then it decreases to one. The real part of at least one eigenvalue is positive during the autocatalytic period as indicated by grey shading

N_s−2-dimensional manifold can be estimated by the distance of the next slowest mode from its equivalent N_s–1 manifold, although there may be some contribution from the faster modes where timescale separation is weak. If N_R is the number of relaxed modes, that is, the number of non-conserved modes that satisfy the relationship $\left|\Delta\widetilde{z}_i\right| < z_{\text{th}}$, then the effective dynamical dimension of the system will be $N_D = N_S - N_C - N_R$.

The calculated N_D is not the actual dimension of the physical or chemical system, but is rather the minimum number of variables that can be used to model the system with acceptable accuracy. For example, a model that is described by an 8-variable ODE, but has dynamical dimension of 2, can be replaced by coupled system of differential and algebraic equations, where the change in values of 2 variables are calculated by ODEs, whilst the values of the other 6 variables can be calculated from these 2 variables using algebraic equations. The actual form of the ODEs or other equivalent time-dependent models can be developed in different ways as will be further discussed in Chap. 7.

Figure 6.6 shows how the dynamical dimension changes during the simulation of an adiabatic explosion of stoichiometric hydrogen−air mixtures ($T_0 = 800$ K, $p = 1$ atm constant). The mechanism contained nine species and 46 irreversible reaction steps. Temperature was also one of the variables of the model. At about $T = 900$ K, the autocatalytic processes become dominant, and therefore, the real part of at least one eigenvalue of the Jacobian becomes positive, and the corresponding mode(s) push the system away from the low-dimensional manifold. After the explosion, the real parts of all eigenvalues become negative, the low-dimensional manifolds become attractive again and the dynamical dimension gradually decreases. Finally, the state of the system approaches the equilibrium point along a 1D manifold.

In Fig. 6.7 some of the trajectories that were shown for the hydrogen flame are now redrawn but coloured according to the estimated dimension of the system at the

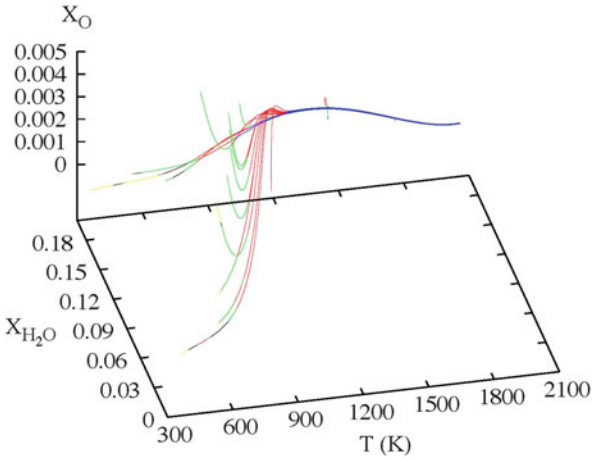

Fig. 6.7 A series of 16 H_2/O_2 flames with the same final equilibrium point are generated from the CHEMKIN program Premix and plotted with a three-dimensional projection. The *colours* indicate the intrinsic dimension calculated according to the use of equation (6-50), $N_D = 1$ (*blue*), $N_D = 2$ (red), $N_D = 3$ (*green*), $N_D = 4$ (*black*) and $N_D = 5$ (*yellow*). Reprinted with permission from Davis and Tomlin (2008a). Copyright (2008) American Chemical Society

particular points in phase space (Davis and Tomlin 2008a). The figure shows the higher intrinsic dimension at the low-temperature points along the trajectories which eventually collapse onto the 1D manifold as the system approaches its adiabatic flame temperature. Therefore, different numbers of variables would be required to model the system depending on whether accurate prediction of the low-temperature region is necessary.

Using the method above, Lovrics et al. (2006) investigated the model of Chen et al. (2000) describing the cell cycle of budding yeast. This model contains 73 parameters and 13 variables. The change in model dimension for a typical time-dependent simulation during a cell division cycle is indicated in Fig. 6.8. During a cycle, the dimension of the model changes between 1 and 7. The dimension increases to seven during the excitation (i.e. autocatalytic) periods and decreases during the relaxation periods. The dimension never reaches zero which would correspond to a stationary state, because the mass of the cell is continuously increasing between two cell divisions, and therefore, the smallest dimension of the model is one. During the period when the dimension is one, the concentrations of the proteins are continuously changing, but the concentrations of all proteins can be calculated from cell mass using algebraic equations. It follows that in order to simulate the whole cycle using a single model, 7 variables may be required in order to be able to capture the excitation periods.

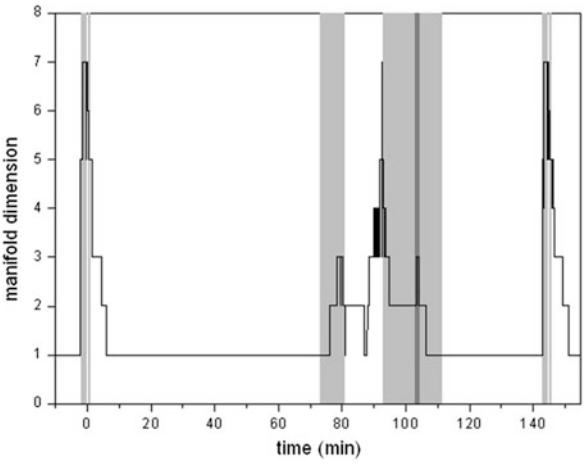

Fig. 6.8 Changes in the dimension of a cell cycle model (Chen et al. 2000) during a whole cell division cycle (from 0 min till 144.92 min). Grey areas indicate time periods where the highest eigenvalue is positive, i.e. periods of autocatalytic changes (Lovrics et al. 2006)

6.6 Timescales in Reactive Flow Models

In a reactive flow system, the chemical timescales should not be treated in isolation from the relevant timescales of the flow processes which may include diffusion, convection/advection or turbulent mixing (Goussis et al. 2005b). The simple initial value problem expressed in Eq. (2.9) must therefore be extended to a system of partial differential equations. Using the notation of Bykov and Maas (2007), the evolution equation for the scalar field of a reacting flow can be described by

$$\frac{\partial \boldsymbol{\psi}}{\partial t} = \mathbf{F}(\boldsymbol{\psi}) - \vec{\boldsymbol{\upsilon}} \cdot \text{grad } \boldsymbol{\psi} + \frac{1}{\rho} \text{div} \mathbf{D} \text{grad } \boldsymbol{\psi} \tag{6.51}$$

where $\boldsymbol{\psi} = (\psi_1, \psi_2, \ldots, \psi_{N_S+2})^T$ is the thermokinetic state, which can, e.g., be expressed by the specific enthalpy h, the pressure P and the mass fractions w_i of the N_S chemical species: $\boldsymbol{\psi} = (h, p, w_1, \ldots, w_{N_S})^T$; $\mathbf{F}$ denotes the chemical source term, $\vec{\boldsymbol{\upsilon}}$ the flow velocity, ρ the density and $\mathbf{D}$ the matrix of transport coefficients. Two limiting cases may exist for the above system of equations. The first is for a well-mixed system where the flow terms are very small compared to the chemical source term. In this case, the last two terms in Eq. (6.51) could be neglected and the equation would return to the homogeneous initial value problem expressed in Eq. (2.9). A slow manifold could therefore be defined based on chemical timescales alone. The second case would be if the chemical source terms were negligible and the process becomes diffusion dominated. An example of this second case might be in the preheating zone of a flame. A discussion of manifolds present for both these limiting cases is given in Bykov and Maas (2007). In general, however, a mixture of chemical and flow timescales will be present within a system which could change over different conditions, e.g. temperatures, composition, etc. Methods which extend chemical slow manifolds into the region of slow chemistry by defining

manifolds governed by only convection and diffusion are likely to neglect regions with strong couplings between the chemical and physical processes (Bykov and Maas 2007, 2009).

Two different approaches have historically been taken to define slow manifolds for such coupled systems. In the first, the governing PDEs are reduced to a system of ordinary differential equations (ODEs), and timescale separation in the resulting ODEs is exploited in order to find underlying slow manifolds (Mengers and Powers 2013). Such Galerkin-based methods are commonly used within numerical algorithms for solving PDEs describing reactive flows, but these will not be the focus of the current discussion. The paper of Mengers and Powers (2013) describes an application of such methods for NO formation during combustion.

In the second approach, the spatially homogeneous chemical slow manifold is used, and the method must somehow account for reaction–transport coupling. For a chemical timescale to be defined as fast in a reactive flow system, the Damköhler number, which is defined as the ratio of the flow timescale τ_f and the chemical timescale τ_c, must be large:

$$Da = \frac{\tau_f}{\tau_c} \gg 1 \tag{6.52}$$

Usually the range of timescales covered by the chemical processes is wider than that covered by transport processes (Maas and Pope 1992b; Davis 2006a). As illustrated in Fig. 6.9, it is common for the fastest chemical timescales to be faster than the relevant transport timescales allowing local equilibrium arguments to be applied to the fast chemistry. However, diffusion processes have been shown in several studies of combustion and enzyme kinetics to affect the use of fast timescale arguments for reduction on a slow manifold constructed according to the chemical kinetics alone (Yannacopoulos et al. 1995; Singh et al. 2002; Davis 2006a).

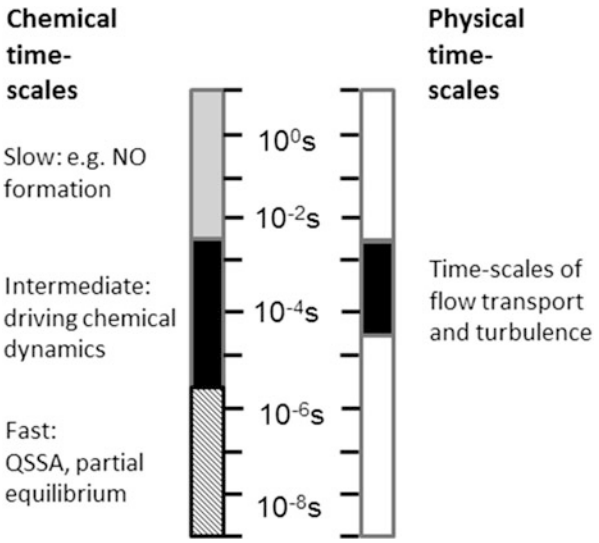

Fig. 6.9 Comparison of chemical versus physical timescales in a typical turbulent combustion system. Adapted from (Maas and Pope 1992b)

The coupling of some chemical modes with relatively fast physical ones may disturb system trajectories from the low-dimensional manifold (Bykov and Maas 2007). Prüfert et al. (2014) provide a discussion of the comparison of species lifetimes τ_i (see Eq. (6.11)), system timescales based on eigenvalues and two additional timescales called system progress and progress variable timescales for reactive flow models.

Yannacopoulos et al. (1995) showed for an enzyme kinetics reaction–diffusion model that because of the spatial dependence of the solution in PDE systems, the transient dynamics before relaxation to the slow chemical manifold can have a very important effect on the solution at long times. The use of a singular perturbation method for the approximation of the transient approach to the slow manifold was seen to improve the simulation of the long-term dynamics of the reaction–diffusion model. A higher-order approximation than the QSSA was also required in order to approximate the slow manifold in this case. Davis et al. (Davis 2006a, b) also showed that the presence of diffusion can affect the attractiveness of the slow manifolds present in a reaction–diffusion model of ozone combustion. The situation for turbulent systems may be even more complex since in such cases rapidly changing transient flows may need to be captured by the reactive flow model. However, Van Oijen et al. (2007) have applied slow manifold techniques even in direct numerical simulations (DNS) of flames. They noted, however, that the 2D slow manifold generated for the flame differed substantially from the one generated based on the chemical kinetics alone. Davis and Tomlin (2008b) also noted differences between the flame manifolds and those based on only chemical kinetics for a hydrogen oxygen flame, when sufficiently far from the final equilibrium point. These differences have been attributed to the influence of the non-invariance of the manifold, the curvature of the manifold (for nonzero diffusion cases), differential diffusion of the species (Ren and Pope 2006) and thermal diffusion (Maas and Bykov 2011). It could be possible to solve such problems by using higher-dimensional chemical manifolds, i.e. only collapsing those timescales which are much faster than the transport ones, but this is not optimal from the point of view of reducing the number of variables to solve for in a reduced model. Therefore, more general approaches have been sought for the application of slow manifolds within reaction–diffusion systems. These include the reaction–diffusion manifold (REDIM) method (Bykov and Maas 2009) and methods based on the extension of composition space to include, for example, diffusive fluxes (Bongers et al. 2002). Both of these approaches will be discussed further in the context of model reduction in Sect. 7.10.

6.7 Stiffness of Reaction Kinetic Models

One of the first applications of computers in science was the simulation of the dislocation of weights interconnected with springs. When the springs were not stiff, the simulation was easy and no numerical problems were encountered. However,

when some springs were loose and the others stiff, the numerical solution was far more difficult, since the ODE solution code only gave sensible results when extremely short time steps were used (Burden and Faires 1993). Physicists called such tasks stiff problems and the corresponding ODE was called a *stiff system of differential equations*. It was subsequently discovered that very similar problems occur not only for the simulation of mechanical problems but also for reaction kinetic models.

The stiffness of a dynamical system can be characterised via its timescales. Remember that the ratio $1/|\mathrm{Re}(\lambda_j)|$ is called the j-th timescale of a dynamical system (see Sect. 6.3). The most widely used *stiffness index* is the reciprocal of the shortest timescale of the system:

$$L = \frac{1}{\min\limits_i \tau_i} = \max_i \frac{1}{\tau_i} = \max_i |\mathrm{Re}\lambda_i| \tag{6.53}$$

where λ_i is the i-th eigenvalue of the Jacobian of the ODE of the system. However, it is only possible to judge if such a quantity is large or small by comparing it to another quantity. The shortest timescale should therefore be compared to the *characteristic timescale* of the system.

Each process has a characteristic timescale. This is the time period during which important events occur that are of interest to us. For example, in the case of a summer storm, the timescale of temperature change is a few hours. During a summer holiday, the change of temperature is of interest over a few weeks, whilst climatologists investigate the change of the average temperature of air for timescales of several thousand or even several million years. In these three cases, the physical system is identical (the atmosphere of Earth), the same quantity (air temperature) is investigated, but the characteristic timescales of the investigations are different.

A model is called stiff if its characteristic time T is several orders of magnitude (typically 8–12 orders of magnitude) longer than its shortest timescale. Stiffness can be characterised by the following *stiffness ratio*:

$$S_1 = \frac{T}{\min\limits_i \tau_i} = LT \tag{6.54}$$

Another possibility is to calculate the ratio of the longest and shortest timescales of the model:

$$S_2 = \frac{\max\limits_i |\mathrm{Re}\lambda_i|}{\min\limits_i |\mathrm{Re}\lambda_i|} \tag{6.55}$$

Of course, zero eigenvalues (originating from the conserved properties of the model) should not be considered.

It is important to emphasise that stiffness belongs to a model and not to a physical system. The same physical system can be described, with similar accuracy, by a very stiff and a non-stiff model. Several mathematics books consider stiffness ratio S_2 as a good indicator for stiffness, but stiffness ratio S_1 is a more realistic characterisation of the stiffness of a physical model. Inserting descriptions of processes that have timescales much longer than the characteristic timescale into a model will not affect the simulations. For example, according to the *pool chemical approximation* (see Sect. 2.3), if the concentration of a species changes negligibly during the simulation, it can be considered constant and the equations can be simplified accordingly. It is clear that adding more, less reactive species to the model (which changes S_2 but not S_1) does not cause much change. In general it may be possible to treat the very slow timescales as approximately conserved variables by applying a threshold ε (i.e. $|\mathrm{Re}\lambda_i| \leq \varepsilon$) and therefore to remove these timescales from the consideration of S_2.

Both stiffness ratios S_1 and S_2 can be decreased by eliminating very fast processes from the model or by changing the corresponding differential equations to algebraic equations. Several sections of the next chapter, dealing with mechanism reduction, discuss methods to modify models so that the fast timescales are eliminated, hence reducing the stiffness of the model, even though the solution of the model on the characteristic timescale is almost identical to the original one. Algorithms for the solution of differential equations can be sorted into many categories, but an important feature from a practical point of view is whether these are applicable for the simulation of stiff systems.

A simple rule of thumb is that *explicit methods for the solution of ODEs* give fast solutions for each time step but are not always applicable for the solution of stiff systems. If an explicit method is used for the simulation of a stiff system using large time steps, the solution obtained is usually not sensible, giving oscillating outputs or the overprediction of quantities. Accuracy and stability problems can be solved by selecting extremely short time steps, but then the overall CPU time required becomes much too long. Using *implicit methods for the solution of ODEs* requires much more CPU time for each time step, but the solution is stable even when using longer time steps.

Explicit methods calculate the solution to Eq. (2.9) at time $t + \Delta t$ knowing the solution at time t using the following general equation:

$$\mathbf{Y}(t + \Delta t) = \mathbf{F}(\mathbf{Y}(t)) \tag{6.56}$$

The general equation for implicit methods contains the solution of the system at both times t and $t + \Delta t$:

$$\mathbf{G}(\mathbf{Y}(t + \Delta t), \mathbf{Y}(t)) = 0 \tag{6.57}$$

Equation (6.57) is a nonlinear algebraic equation. Solving it at each time step Δt would require much CPU time, and so it is converted to an approximate linear algebraic equation.

When an explicit method is used, the solution $\mathbf{Y}$ at time t is fed into Eq. (6.56) to get the solution at time $t + \Delta t$. Using an implicit method, the Jacobian has to be evaluated at each time step, and then using this matrix, an N-variable linear algebraic system of equations has to be solved. If using the same time step Δt for both methods, the implicit method will require more CPU time unless highly efficient matrix algebra techniques can be employed. If the ODE is not stiff, then both explicit and implicit methods give an accurate solution. If the ODE is stiff, then the explicit method will not give sensible results for large time steps Δt, whilst the implicit method may give an accurate numerical solution. This means that if the ODE is not stiff, then it is usually not practical (although possible) to use an implicit method. For the solution of a stiff ODE, it may be more practical to use an implicit method, although the use of variable time steps can improve the efficiency of explicit schemes (Sandu et al. 1997b).

A full discussion of the issues involved and comparisons between the applications of explicit and implicit solvers to five test problems from atmospheric chemistry is given by Sandu et al. (1997a, b). Typically, the stiffness ratio for these types of problems is between 10^6 and 10^9, and therefore, they pose significant numerical challenges for long timescale tropospheric modelling. All test cases were simulated for 5 days with a required accuracy of 1 %. The chemical schemes were of varying dimensions and in one test case, liquid-phase chemistry and gas–liquid interactions were included. A range of variable time-step explicit and implicit schemes were tested, as well as schemes which utilised solutions based on the QSSA for species with very short lifetimes. For low-dimensional problems, the best of the implicit solvers outperformed the best of the explicit schemes in terms of CPU time required for a given accuracy. For larger-dimensional problems, the implicit schemes outperformed the explicit ones if higher accuracy was required. However, sparse linear algebra implementations were necessary in order to avoid large increases in the CPU requirements for the implicit methods, due to their requirement for Jacobian manipulations. In most cases, the QSSA-based schemes performed the worst. Explicit methods were found to be unsuitable for the test case involving liquid-phase chemistry due to the large stiffness ratio present in this problem. One feature which is notable from this study is that the simple rule of thumb, which was introduced at the beginning of this section, may not be so simple, when variable time-stepping, sparse linear algebra and efficient iterative methods are taken into account. Depending on the dimension of the problem and the accuracy required, the relative performance of the explicit and implicit schemes can vary. Sandu et al. recommend the optimisation of different solvers for individual applications and in fact offer users the opportunity to automatically select solvers for each simulation case using their symbolic chemical preprocessor KPP (Damian et al. 2002; KPP; Sandu et al. 2003; Daescu et al. 2003). Readers who are particularly interested in optimising solution methods for stiff chemical systems are recommended to study these benchmarking tests and to try their own problem!

There are several other points that should be kept in mind when the simulation of stiff models is dealt with. In science (physics, chemistry, biology), almost all

models based on differential equations are likely to be stiff, because the models have to take into account much faster processes than the characteristic time of the simulated system. However, in most practical cases, the modeller does not have to investigate the stiffness of the model, because modern ODE solvers select an explicit method for a non-stiff and an appropriate implicit method for a stiff problem. These solvers may select a different method if the stiffness of the system changes significantly during the simulation.

Almost all simulation codes require acceptable stepwise absolute and relative error thresholds as inputs. This is important because it allows the algorithm to use a variable stepsize and to calculate the largest Δt that allows the predicted error to be within the error thresholds. Using an explicit algorithm for the solution of a stiff ODE, the estimated time step Δt may be several orders of magnitude (e.g. 10^8 times) smaller than the characteristic time, whilst using an implicit method Δt is typically only 2–3 orders of magnitude smaller than the characteristic time. However, implicit methods carry the extra burden of the linear algebra required due to Jacobian manipulations. Sparse linear algebra methods can lead to big efficiency gains for higher-dimensional problems (Sandu et al. 1997b).

Both explicit and implicit methods have many variations. One of the differences between these methods is the order of the polynomial that is used for the approximation of the solution. The more sophisticated methods provide more accurate solutions, but the most important is to use a temporal and/or spatial stepsize that allows the stability of the method (Higham 1996).

6.8 Operator Splitting and Stiffness

The main discussion of the book is restricted to the solution of ordinary differential equations (ODEs) which describe the chemical changes in a model. Many situations involve not only chemical processes but also physical ones, such as convection/advection, diffusion, turbulent mixing, etc., as described in Sect. 6.6. The discussion of solution methods for the partial differential equations (PDEs) that result from the inclusion of such physical processes is beyond the scope of this book. However, it is worthwhile to mention some issues here which relate to timescales and the inherent stiffness of PDE models, and how these may affect the choice of solution method. Using the more traditional method of lines approach, the PDEs are discretised in space only, transforming the PDEs into a set of ODEs for the variables at the grid nodes. For stiff systems, this may have to be coupled with the use of an implicit numerical scheme for the time integration, leading to a large number of algebraic manipulations, since the size of the matrices to be inverted is determined by the square of the number of chemical species multiplied by the number of grid cells. Therefore, usually either chemical detail or grid resolution has to be sacrificed in order to keep the computational times practical for spatially 2D or 3D models.

In many situations, the method of *operator splitting* is applied to the solution of PDEs. In this case, the chemical kinetic step is separated from the transport steps and solved using ODE methods as described above. One of the advantages of operator splitting is that by separating the original convection–reaction–diffusion PDEs into different steps, it is possible to optimise solution methods that have been specifically developed for each submodel. Even if an implicit method has to be used for the chemical part, the matrices are far smaller than those resulting from the method of lines approach.

Splitting methods have been successfully applied in atmospheric chemical systems (Sportisse 2000) as well as in combustion where the applicability of splitting may be less obvious since the chemistry feeds back to the transport terms through heat release (Yang and Pope 1998; Knio et al. 1999; Schwer et al. 2003; Singer et al. 2006; Ren and Pope 2008). Discussions on the use of operator splitting in biochemical and developmental biology systems are also given in Logist et al. (2009), Zhu et al. (2009) and Zhao et al. (2011). Stiffness, however, does pose some problems for controlling errors due to operator splitting as investigated by Sportisse using singular perturbation methods (Sportisse 2000). Berkenbosch et al. discussed similar issues for detonation problems in combustion (Berkenbosch et al. 1998), which contain a wide range of timescales. Sportisse suggests that the order of the operator sequence is critical for stiff problems with the stiff operator being applied last for any time step. This ensures that the solution relaxes back to the underlying slow manifold at the end of the overall time step, even though certain sub-steps (e.g. diffusion) may take the solution trajectory away from the manifold. Yang and Pope (1998) suggest coupling operator splitting techniques with solutions of the chemical system on the slow manifold in order to overcome some of these problems. Valorani and Goussis introduce a solution algorithm based on splitting the slow and fast timescales using CSP and using an explicit solver for the slow variables with the contribution of the fast variables taken into account at the end of each integration step as a correction (Valorani and Goussis 2001). Tomlin et al. (1997) discuss the application of operator splitting at the level of the nonlinear equations resulting from the discretisation of the PDE using the method of lines, rather than at the level of the PDE itself. The splitting is then applied to the approximation of the Jacobian of the full system (Berzins and Ware 1996) which reduces the size of the matrices to be inverted. In this case, the splitting affects only the rate of convergence of the solution rather than the solution accuracy.

In summary, without the use of operator splitting at some level, the discretisation of a full PDE system containing a very large detailed chemical mechanism can lead to the use of implicit methods handling very large equation systems. This is a numerically challenging task that could perhaps be handled using state-of-the-art linear algebra techniques. However, for stiff systems, care must be taken in how the splitting algorithm is designed.

References

Adrover, A., Creta, F., Giona, M., Valorani, M., Vitacolonna, V.: Natural tangent dynamics with recurrent biorthonormalizations: a geometric computational approach to dynamical systems exhibiting slow manifolds and periodic/chaotic limit sets. Physica D **213**, 121–146 (2006)

Bell, N., Heard, D.E., Pilling, M.J., Tomlin, A.S.: Atmospheric lifetime as a probe of radical chemistry in the boundary layer. Atmos. Environ. **37**, 2193–2205 (2003)

Berkenbosch, A.C., Kaasschieter, E.F., Klein, R.: Detonation capturing for stiff combustion chemistry. Combust. Theory Model. **2**, 313–348 (1998)

Berzins, M., Ware, J.M.: Solving convection and convection-reaction problems using the method of lines. Appl. Numer. Math. **20**, 83–99 (1996)

Blasenbrey, T.: Entwicklung und Implementierung automatisch reduzierter Reaktionsmechanismen für die Verbrennung von Kohlenwasserstoffen. Stuttgart University (2000)

Bongers, H., Van Oijen, J.A., De Goey, L.P.H.: Intrinsic low-dimensional manifold method extended with diffusion. Proc. Combust. Inst. **29**, 1371–1378 (2002)

Büki, A., Perger, T., Turányi, T., Maas, U.: Repro-modelling based generation of intrinsic low-dimensional manifolds. J. Math. Chem. **31**, 345–362 (2002)

Burden, R.L., Faires, J.D.: Numerical Analysis, 5th edn. Prindle, Weber and Schmidt, Boston (1993)

Bykov, V., Maas, U.: The extension of the ILDM concept to reaction-diffusion manifolds. Combust. Theory Model. **11**, 839–862 (2007)

Bykov, V., Maas, U.: Problem adapted reduced models based on reaction-diffusion manifolds (REDIMs). Proc. Combust. Inst. **32**, 561–568 (2009)

Chen, C.C., Csikász-Nagy, A., Győrffy, B., Val, J., Novák, B., Tyson, J.J.: Kinetic analysis of a molecular model of the budding yeast cell cycle. Mol. Biol. Cell **11**, 369–391 (2000)

Daescu, D., Sandu, A., Carmichael, G.R.: Direct and adjoint sensitivity analysis of chemical kinetic systems with KPP: Part II—Validation and numerical experiments. Atmos. Environ. **37**, 5097–5114 (2003)

Damian, V., Sandu, A., Damian, M., Potra, F., Carmichael, G.R.: The kinetic PreProcessor KPP—a software environment for solving chemical kinetics. Comp. Chem. Eng. **26**, 1567–1579 (2002)

Davis, M.J.: Low-dimensional manifolds in reaction−diffusion equations. 1. Fundamental aspects. J. Phys. Chem. A **110**, 5235–5256 (2006a)

Davis, M.J.: Low-dimensional manifolds in reaction−diffusion equations. 2. Numerical analysis and method development. J. Phys. Chem. A **110**, 5257–5272 (2006b)

Davis, M.J., Tomlin, A.S.: Spatial dynamics of steady flames 1. Phase space structure and the dynamics of individual trajectories. J. Phys. Chem. A **112**, 7768–7783 (2008a)

Davis, M.J., Tomlin, A.S.: Spatial dynamics of steady flames 2. Low-dimensional manifolds and the role of transport processes. J. Phys. Chem. A **112**, 7784–7805 (2008b)

Di Carlo, P., Brune, W.H., Martinez, M., Harder, H., Lesher, R., Ren, X.R., Thornberry, T., Carroll, M.A., Young, V., Shepson, P.B., Riemer, D., Apel, E., Campbell, C.: Missing OH reactivity in a forest: evidence for unknown reactive biogenic VOCs. Science **304**, 722–725 (2004)

Fenichel, N.: Geometric singular perturbation theory for ordinary differential equations. J. Diff. Equations **31**, 53–98 (1979)

Fotache, C.G., Kreutz, T.G., Law, C.K.: Ignition of counterflowing methane versus heated air under reduced and elevated pressures. Combust. Flame **108**, 442–470 (1997)

García-Ybarra, P.L., Treviño, C.: Asymptotic analysis of the boundary layer H_2 ignition by a hot flat plate with thermal diffusion. Combust. Flame **96**, 293–303 (1994)

Goussis, D.A.: On the construction and use of reduced chemical kinetic mechanisms produced on the basis of given algebraic relations. J. Comput. Phys. **128**, 261–273 (1996)

Goussis, D.A., Lam, S.H.: A study of homogeneous methanol oxidation kinetics using CSP. Proc. Combust. Inst. **24**, 113–120 (1992)

Goussis, D.A., Najm, H.N.: Model reduction and physical understanding of slowly oscillating processes: the circadian cycle. SIAM Multiscale Model. Simul. **5**, 1297–1332 (2006)
Goussis, D.A., Skevis, G.: Nitrogen chemistry controlling steps in methane-air premixed flames. In: Bathe, K.J. (ed.) Computational Fluid and Solid Mechanics, pp. 650–653. Elsevier, Amsterdam (2005)
Goussis, D.A., Valorani, M., Creta, F., Najm, H.N.: In: Bathe, K. (ed.) Computational Fluid and Solid Mechanics, vol. 2. Elsevier, Amsterdam, pp. 1951–1954 (2003)
Goussis, D.A., Skevis, G., Mastorakos, E.: Transport-chemistry interactions in laminar premixed hydrogen-air flames near flammability limits. Proceedings of ECM (2005a)
Goussis, D.A., Valorani, M., Creta, F., Najm, H.N.: Reactive and reactive-diffusive time scales in stiff reaction-diffusion systems. Prog. Comput. Fluid Dyn. **5**, 316–326 (2005b)
Gupta, S., Im, H.G., Valorani, M.: Classification of ignition regimes in HCCI combustion using computational singular perturbation. Proc. Combust. Inst. **33**, 2991–2999 (2011)
Hadjinicolaou, M., Goussis, D.A.: Asymptotic solution of stiff PDEs with the CSP method: the reaction diffusion equation. SIAM J. Sci. Comput. **20**, 781–810 (1998)
Herbinet, O., Pitz, W., Westbrook, C.K.: Detailed chemical kinetic mechanism for the oxidation of biodiesel fuels blend surrogate. Combust. Flame **157**, 893–908 (2010)
Hesstvedt, E., Hov, O., Isaksen, I.S.A.: Quasi-steady-state approximations in air-pollution modeling—comparison of two numerical schemes for oxidant prediction. Int. J. Chem. Kinet. **10**, 971–994 (1978)
Higham, N.J.: Accuracy and Stability of Numerical Algorithms. SIAM, Philadelphia (1996)
Ingham, T., Goddard, A., Whalley, L.K., Furneaux, K.L., Edwards, P.M., Seal, C.P., Self, D.E., Johnson, G.P., Read, K.A., Lee, J.D., Heard, D.E.: A flow-tube based laser-induced fluorescence instrument to measure OH reactivity in the troposphere. Atmos. Meas. Tech. **2**, 465–477 (2009)
Klonowski, W.: Simplifying principles for chemical and enzyme reaction kinetics. Biophys. Chem. **18**, 73–87 (1983)
Knio, O.M., Najm, H.N., Wyckoff, P.S.: A semi-implicit numerical scheme for reacting flow II. Stiff, operator-split formulation. J. Comput. Phys. **154**, 428–467 (1999)
Kourdis, P.D., Goussis, D.A.: Glycolysis in saccharomyces cerevisiae: algorithmic exploration of robustness and origin of oscillations. Math. Biosci. **243**, 190–214 (2013)
Kourdis, P.D., Steuer, R., Goussis, D.A.: Physical understanding of complex multiscale biochemical models via algorithmic simplification: glycolysis in *Saccharomyces cerevisiae*. Physica D **239**, 1798–1817 (2010)
Kovacs, T.A., Brune, W.H.: Total OH loss rate measurement. J. Atmos. Chem. **39**, 105–122 (2001)
KPP: Kinetic Preprocessor. http://people.cs.vt.edu/~asandu/Software/Kpp/
Kremling, A., Fischer, S., Sauter, T., Bettenbrock, K., Gilles, E.D.: Time hierarchies in the *Escherichia coli* carbohydrate uptake and metabolism. Biosystems **73**, 57–71 (2004)
Lam, S.H.: Using CSP to understand complex chemical kinetics. Combust. Sci. Technol. **89**, 375–404 (1993)
Lam, S.H.: Reduced chemistry-diffusion coupling. Combust. Sci. Technol. **179**, 767–786 (2006)
Lam, S.H.: Model reductions with special CSP data. Combust. Flame **160**, 2707–2711 (2013)
Lam, S.H., Goussis, D.A.: Understanding complex chemical kinetics with computational singular perturbation. Proc. Combust. Inst. **22**, 931–941 (1988)
Lam, S.H., Goussis, D.A.: Conventional asymptotics and computational singular perturbation for simplified kinetics modeling. In: Smooke, M.O. (ed.) Reduced Kinetic Mechanisms and Asymptotic Approximations for Methane-Air Flames. Springer Lecture Notes, vol. 384, pp. 227–242. Springer, Berlin (1991)
Lam, S.H., Goussis, D.A.: The CSP method for simplifying kinetics. Int. J. Chem. Kinet. **26**, 461–486 (1994)
Lee, C.H., Othmer, H.G.: A multi-time-scale analysis of chemical reaction networks: I. Deterministic systems. J. Math. Biol. **60**, 387–450 (2010)

Lee, J.C., Najm, H.N., Lefantzi, S., Ray, J., Frenklach, M., Valorani, M., Goussis, D.: On chain branching and its role in homogeneous ignition and premixed flame propagation. In: Bathe, K. (ed.) Computational Fluid and Solid Mechanics, pp. 717–720. Elsevier, Amsterdam (2005)

Lee, J.C., Najm, H.N., Lefantzi, S., Ray, J., Frenklach, M., Valorani, M., Goussis, D.: A CSP and tabulation-based adaptive chemistry model. Combust. Theory Model. **11**, 73–102 (2007)

Lee, J.D., Young, J.C., Read, K.A., Hamilton, J.F., Hopkins, J.R., Lewis, A.C., Bandy, B.J., Davey, J., Edwards, P., Ingham, T., Self, D.E., Smith, S.C., Pilling, M.J., Heard, D.E.: Measurement and calculation of OH reactivity at a United Kingdom coastal site. J. Atmos. Chem. **64**, 53–76 (2009)

Logist, F., Saucez, P., Van Impe, J., Wouwer, A.V.: Simulation of (bio)chemical processes with distributed parameters using Matlab (R). Chem. Eng. J. **155**, 603–616 (2009)

Løvås, T., Amneus, P., Mauss, F., Mastorakos, E.: Comparison of automatic reduction procedures for ignition chemistry. Proc. Combust. Inst. **29**, 1387–1393 (2002)

Løvås, T., Mastorakos, E., Goussis, D.A.: Reduction of the RACM scheme using computational singular perturbation analysis. J. Geophys. Res. Atmos. **111**(D13302) (2006)

Lovrics, A., Csikász-Nagy, A., Zsély, I.G., Zádor, J., Turányi, T., Novák, B.: Time scale and dimension analysis of a budding yeast cell cycle model. BMC Bioinform. **7**, 494 (2006)

Lu, T., Law, C.K.: A criterion based on computational singular perturbation for the identification of quasi steady state species: a reduced mechanism for methane oxidation with NO chemistry. Combust. Flame **154**, 761–774 (2008a)

Lu, T., Law, C.K.: Strategies for mechanism reduction for large hydrocarbons: *n*-heptane. Combust. Flame **154**, 153–163 (2008b)

Lu, T., Ju, Y., Law, C.K.: Complex CSP for chemistry reduction and analysis. Combust. Flame **126**, 1445–1455 (2001)

Lu, T.F., Yoo, C.S., Chen, J.H., Law, C.K.: Three-dimensional direct numerical simulation of a turbulent lifted hydrogen jet flame in heated coflow: a chemical explosive mode analysis. J. Fluid Mech. **652**, 45–64 (2010)

Luo, Z., Yoo, C.S., Richardson, E.S., Chen, J.H., Law, C.K., Lu, T.F.: Chemical explosive mode analysis for a turbulent lifted ethylene jet flame in highly-heated coflow. Combust. Flame **159**, 265–274 (2012c)

Maas, U.: Coupling of chemical reaction with flow and molecular transport. Appl. Math. **40**, 249–266 (1995)

Maas, U.: Efficient calculation of intrinsic low-dimensional manifolds for the simplification of chemical kinetics. Comput. Vis. Sci. **1**, 69–81 (1998)

Maas, U.: Mathematical modeling of the coupling of chemical kinetics with flow and molecular transport. In: Keil, F., Mackens, W., Voss, H., Werther, J. (eds.) Scientific Computing in Chemical Engineering II, pp. 26–56. Springer, Berlin (1999)

Maas, U., Bykov, V.: The extension of the reaction/diffusion manifold concept to systems with detailed transport models. Proc. Combust. Inst. **33**, 1253–1259 (2011)

Maas, U., Pope, S.B.: Implementation of simplified chemical kinetics based on intrinsic low-dimensional manifolds. Proc. Combust. Inst. **24**, 103–112 (1992a)

Maas, U., Pope, S.B.: Simplifying chemical kinetics: intrinsic low-dimensional manifolds in composition space. Combust. Flame **88**, 239–264 (1992b)

Maas, U., Pope, S.B.: Laminar flame calculations using simplified chemical kinetics based on intrinsic low-dimensional manifolds. Proc. Combust. Inst. **25**, 1349–1356 (1994)

Maas, U., Thévenin, D.: Correlation analysis of direct numerical simulation data of turbulent non-premixed flames. Proc. Combust. Inst. **27**, 1183–1189 (1998)

Maas, U., Warnatz, J.: Ignition processes in hydrogen-oxigen mixtures. Combust. Flame **74**, 53–69 (1988)

Macken, K.V., Sidebottom, H.W.: The reactions of methyl radicals with chloromethanes. Int. J. Chem. Kinet. **11**, 511–527 (1979)

Mao, J., Ren, X., Brune, W.H., Olson, J.R., Crawford, J.H., Fried, A., Huey, L.G., Cohen, R.C., Heikes, B., Singh, H.B., Blake, D.R., Sachse, G.W., Diskin, G.S., Hall, S.R., Shetter, R.E.:

Airborne measurement of OH reactivity during INTEX-B. Atmos. Chem. Phys. **9**, 163–173 (2009)
Massias, A., Diamantis, D., Mastorakos, E., Goussis, D.A.: An algorithm for the construction of global reduced mechanisms with CSP data. Combust. Flame **117**, 685–708 (1999a)
Massias, A., Diamantis, D., Mastorakos, E., Goussis, D.A.: Global reduced mechanisms for methane and hydrogen combustion with nitric oxide formation constructed with CSP data. Combust. Theory Model. **3**, 233–257 (1999b)
Mengers, J.D., Powers, J.M.: One-dimensional slow invariant manifolds for fully coupled reaction and micro-scale diffusion. SIAM J. Appl. Dyn. Syst. **12**, 560–595 (2013)
Mittal, G., Chaos, M., Sung, C.J., Dryer, F.L.: Dimethyl ether autoignition in a rapid compression machine: experiments and chemical kinetic modeling. Fuel Process. Technol. **89**, 1244–1254 (2008)
Mora-Ramirez, M.A., Velasco, R.M.: Reduction of CB05 mechanism according to the CSP method. Atmos. Environ. **45**, 235–243 (2011)
Nagy, T., Turányi, T.: Relaxation of concentration perturbation in chemical kinetic systems. Reac. Kinet. Catal. Lett. **96**, 269–278 (2009)
Neophytou, M.K., Goussis, D.A., van Loon, M., Mastorakos, E.: Reduced chemical mechanisms for atmospheric pollution using computational singular perturbation analysis. Atmos. Environ. **38**, 3661–3673 (2004)
Nicolini, P., Frezzato, D.: Features in chemical kinetics. I. Signatures of self-emerging dimensional reduction from a general format of the evolution law. J. Chem. Phys. **138**(234101) (2013a)
Nicolini, P., Frezzato, D.: Features in chemical kinetics. II. A self-emerging definition of slow manifolds. J. Chem. Phys. **138**(234102) (2013b)
Pilling, M.J., Seakins, P.W.: Reaction Kinetics. Oxford University Press, Oxford (1995)
Pontryagin, L.S.: Ordinary Differential Equations. Elsevier, Amsterdam (1962)
Prager, J., Najm, H.N., Valorani, M., Goussis, D.A.: Skeletal mechanism generation with CSP and validation for premixed n-heptane flames. Proc. Combust. Inst. **32**, 509–517 (2009)
Prasolov, V.V.: Problems and Theorems in Linear Algebra. Translations of Mathematical Monographs, vol. 134. American Mathematical Society, Cambridge (1994)
Prüfert, U., Hunger, F., Hasse, C.: The analysis of chemical time scales in a partial oxidation flame. Combust. Flame **161**, 416–426 (2014)
Ren, Z., Pope, S.B.: The use of slow manifolds in reactive flows. Combust. Flame **147**, 243–261 (2006)
Ren, Z.Y., Pope, S.B.: Second-order splitting schemes for a class of reactive systems. J. Comput. Phys. **227**, 8165–8176 (2008)
Roussel, M.R., Fraser, S.J.: Accurate steady-state approximation: implications for kinetics experiments and mechanism. J. Chem. Phys. **94**, 7106–7113 (1991)
Sandu, A., Verwer, J.G., Blom, J.G., Spee, E.J., Carmichael, G.R., Potra, F.A.: Benchmarking stiff ODE solvers for atmospheric chemistry problems II: Rosenbrock solvers. Atmos. Environ. **31**, 3459–3472 (1997a)
Sandu, A., Verwer, J.G., Van Loon, M., Carmichael, G.R., Potra, F.A., Dabdub, D., Seinfeld, J.H.: Benchmarking stiff ODE solvers for atmospheric chemistry problems I. implicit vs. explicit. Atmos. Environ. **31**, 3151–3166 (1997b)
Sandu, A., Daescu, D.N., Carmichael, G.R.: Direct and adjoint sensitivity analysis ofchemical kinetic systems with KPP: Part I – theory and software tools. Atmos. Environ. **37**, 5083–5096 (2003)
Schwer, D.A., Lu, P., Green, W.H., Semiao, V.: A consistent-splitting approach to computing stiff steady-state reacting flows with adaptive chemistry. Combust. Theory Model. **7**, 383–399 (2003)
Scott, S.K.: Chemical Chaos. International Series of Monographs on Chemistry, vol. 24. Clarendon Press, Oxford (1990)

Singer, M.A., Pope, S.B., Najm, H.N.: Operator-splitting with ISAT to model reacting flow with detailed chemistry. Combust. Theory Model. **10**, 199–217 (2006)
Singh, S., Powers, J.M., Paolucci, S.: On slow manifolds of chemically reactive systems. J. Chem. Phys. **117**, 1482–1496 (2002)
Sportisse, B.: An analysis of operator splitting techniques in the stiff case. J. Comput. Phys. **161**, 140–168 (2000)
Tomlin, A., Berzins, M., Ware, J., Smith, J., Pilling, M.J.: On the use of adaptive gridding methods for modelling chemical transport from multi-scale sources. Atmos. Environ. **31**, 2945–2959 (1997)
Tomlin, A.S., Whitehouse, L., Lowe, R., Pilling, M.J.: Low-dimensional manifolds in tropospheric chemical systems. Faraday Discuss. **120**, 125–146 (2001)
Treviño, C.: Ignition phenomena in H_2/O_2 mixtures. Prog. Astronaut. Aeronautics **131**, 19–43 (1991)
Treviño, C., Liñan, A.: Mixing layer ignition of hydrogen. Combust. Flame **103**, 129–141 (1995)
Treviño, C., Mendez, F.: Asymptotic analysis of the ignition of hydrogen by a hot plate in a boundary layer flow. Combust. Sci. Technol. **78**, 197–216 (1991)
Treviño, C., Mendez, F.: Reduced kinetic mechanism for methane ignition. Proc. Combust. Inst. **24**, 121–127 (1992)
Treviño, C., Solorio, F.: Asymptotic analysis of high temperature ignition of $CO/H_2/O_2$ mixtures. Combust. Flame **86**, 285–295 (1991)
Turányi, T., Tomlin, A.S., Pilling, M.J.: On the error of the quasi-steady-state approximation. J. Phys. Chem. **97**, 163–172 (1993)
Valorani, M., Goussis, D.A.: Explicit time-scale splitting algorithm for stiff problems: auto-ignition of gaseous mixtures behind a steady shock. J. Comput. Phys. **169**, 44–79 (2001)
Valorani, M., Najm, H.N., Goussis, D.A.: CSP analysis of a transient flame-vortex interaction: time scales and manifolds. Combust. Flame **134**, 35–53 (2003)
Valorani, M., Creta, F., Goussis, D.A., Najm, H.N., Lee, J.C.: Chemical kinetics mechanism simplification via CSP. In: Bathe, K.J. (ed.) Computational Fluid and Solid Mechanics, pp. 900–904. Elsevier, Amsterdam (2005a)
Valorani, M., Goussis, D.A., Creta, F., Najm, H.N.: Higher order corrections in the approximation of low dimensional manifolds and the construction of simplified problems with the CSP method. J. Comput. Phys. **209**, 754–786 (2005b)
Valorani, M., Creta, F., Goussis, D., Lee, J., Najm, H.: An automatic procedure for the simplification of chemical kinetic mechanisms based on CSP. Combust. Flame **146**, 29–51 (2006)
Valorani, M., Creta, F., Donato, F., Najm, H.N., Goussis, D.A.: Skeletal mechanism generation and analysis for *n*-heptane with CSP. Proc. Combust. Inst. **31**, 483–490 (2007)
Van Oijen, J.A., Bastlaans, R.J.M., De Goey, L.P.H.: Low-dimensional manifolds in direct numerical simulations of premixed turbulent flames. Proc. Combust. Inst. **31**, 1377–1384 (2007)
Westbrook, C.K., Naik, C.V., Herbinet, O., Pitz, W.J., Mehl, M., Sarathy, S.M., Curran, H.J.: Detailed chemical kinetic reaction mechanisms for soy and rapeseed biodiesel fuels. Combust. Flame **158**, 742–755 (2011)
Yang, B., Pope, S.B.: An investigation of the accuracy of manifold methods and splitting schemes in the computational implementation of combustion chemistry. Combust. Flame **112**, 16–32 (1998)
Yannacopoulos, A.N., Tomlin, A.S., Brindley, J., Merkin, J.H., Pilling, M.J.: The use of algebraic sets in the approximation of inertial manifolds and lumping in chemical kinetic systems. Physica D **83**, 421–449 (1995)
Zagaris, A., Kaper, H.G., Kaper, T.J.: Analysis of the computational singular perturbation reduction method for chemical kinetics. J. Nonlinear Sci. **14**, 59–91 (2004)

Zhao, S., Ovadia, J., Liu, X., Zhang, Y.-T., Nie, Q.: Operator splitting implicit integration factor methods for stiff reaction-diffusion-advection systems. J. Comput. Phys. **230**, 5996–6009 (2011)

Zhu, J., Zhang, Y.-T., Newman, S., Alber, M.: Application of discontinuous Galerkin methods for reaction-diffusion systems in developmental biology. J. Sci. Comput. **40**, 391–418 (2009)

Zsély, I.G., Zádor, J., Turányi, T.: On the similarity of the sensitivity functions of methane combustion models. Combust. Theory Model. **9**, 721–738 (2005)